

Rothamsted Repository Download

A - Papers appearing in refereed journals

Xu, H., Curtis, T. Y., Powers, S. J., Raffan, S., Gao, R., Huang, J., Heiner, M., Gilbert, D. R. and Halford, N. G. 2018. Genomic, biochemical and modelling analyses of asparagine synthetases from wheat. *Frontiers in Plant Science*. 8, p. 2237.

The publisher's version can be accessed at:

- <https://dx.doi.org/10.3389/fpls.2017.02237>

The output can be accessed at: <https://repository.rothamsted.ac.uk/item/84611/genomic-biochemical-and-modelling-analyses-of-asparagine-synthetases-from-wheat>.

© 15 January 2018, Please contact library@rothamsted.ac.uk for copyright queries.

Genomic, biochemical and modelling analyses of asparagine synthetases from wheat

Hongwei Xu^{1,2}, Tanya Y. Curtis¹, Stephen J. Powers³, Sarah Raffan¹, Runhong Gao^{2,1}, Jianhua Huang², Monika Heiner⁴, David R. Gilbert⁵, Nigel G. Halford^{1*}

¹Plant Science, Rothamsted Research, United Kingdom, ²Biotechnology Research Institute, Shanghai Academy of Agricultural Sciences, China, ³Computational and Analytical Sciences Department, Rothamsted Research, United Kingdom, ⁴Department of Computer Science, Brandenburg Technical University, Germany, ⁵College of Engineering, Design and Physical Sciences, Brunel University London, United Kingdom

Submitted to Journal:
Frontiers in Plant Science

Specialty Section:
Plant Physiology

Article type:
Original Research Article

Manuscript ID:
278898

Received on:
04 Sep 2017

Revised on:
05 Dec 2017

Frontiers website link:
www.frontiersin.org

Conflict of interest statement

The authors declare a potential conflict of interest and state it below

The project was part-funded by a consortium of companies and organisations from the wheat supply chain

Author contribution statement

HX. Molecular cloning, expression and biochemical analysis of wheat asparagine synthetases

TYC. Modelling

SJP. Statistical analyses

SR. Genomic analyses

RG. Nucleotide sequence analysis of wheat asparagine synthetases

JH. Joint project leader

MH. Modelling

DG. Modelling

NGH. Joint project leader and lead author

Keywords

wheat, asparagine synthetase, Acrylamide, Food Safety, enzyme activity, mathematical modelling

Abstract

Word count: 350

Asparagine synthetase activity in cereals has become an important issue with the discovery that free asparagine concentration determines the potential for formation of acrylamide, a probably carcinogenic processing contaminant, in baked cereal products. Asparagine synthetase catalyses the ATP-dependent transfer of the amino group of glutamine to a molecule of aspartate to generate glutamate and asparagine. Here, asparagine synthetase-encoding polymerase chain reaction products were amplified from wheat (*Triticum aestivum*) cv. Spark cDNA. The encoded proteins were assigned the names TaASN1, TaASN2 and TaASN3 on the basis of comparisons with other wheat and cereal asparagine synthetases. Although very similar to each other they differed slightly in size, with molecular masses of 65.49, 65.06 and 66.24 kDa, respectively. Chromosomal positions and scaffold references were established for TaASN1, TaASN2 and TaASN3, and a fourth, more recently identified gene, TaASN4. TaASN1, TaASN2 and TaASN4 were all found to be single copy genes, located on Chromosomes 5, 3 and 4, respectively, of each genome (A, B and D), although variety Chinese Spring lacked a TaASN2 gene in the B genome. Two copies of TaASN3 were found on Chromosome 1 of each genome, and these were given the names TaASN3.1 and TaASN3.2. The TaASN1, TaASN2 and TaASN3 PCR products were heterologously-expressed in *Escherichia coli* (TaASN4 was not investigated in this part of the study). Western blot analysis identified two monoclonal antibodies that recognised the three proteins, but did not distinguish between them, despite being raised to epitopes SKKPRMIEVAAP and GGSNKPGVMNTV in the variable C-terminal regions of the proteins. The heterologously-expressed TaASN1 and TaASN2 proteins were found to be active asparagine synthetases, producing asparagine and glutamate from glutamine and aspartate. The asparagine synthetase reaction was modelled using SNOOPY® software and information from the BRENDA database to generate differential equations to describe the reaction stages, based on mass action kinetics. Experimental data from the reactions catalysed by TaASN1 and TaASN2 were entered into the model using Copasi, enabling values to be determined for kinetic parameters. Both the reaction data and the modelling showed that the enzymes continued to produce glutamate even when the synthesis of asparagine had ceased due

Funding statement

HX and RG were supported as visiting workers at Rothamsted Research by Shanghai Agriculture Applied Technology Development Program, China (Grant No. Z20160101) and overseas visiting grants from Shanghai Academy of Agricultural Sciences, Shanghai, Peoples' Republic of China. TYC was supported by the Biotechnology and Biological Sciences Research Council (BBSRC) of the United Kingdom and a consortium of companies and organisations from the wheat supply chain through stand-alone LINK project 'Genetic improvement of wheat to reduce the potential for acrylamide formation during processing'. NGH was supported at Rothamsted Research by the BBSRC via the 20:20 Wheat® and Designing Future Wheat Programmes.

Ethics statements

(Authors are required to state the ethical considerations of their study in the manuscript, including for cases where the study was exempt from ethical approval procedures)

Does the study presented in the manuscript involve human or animal subjects: No

In review

Genomic, biochemical and modelling analyses of asparagine synthetases from wheat

Hongwei Xu^{1,2}, Tanya Y. Curtis², Stephen J. Powers³, Sarah Raffan², Runhong Gao^{1,2}, Jianhua Huang^{1}, Monika Heiner⁴, David Gilbert⁵ and Nigel G. Halford^{2*}*

¹Biotechnology Research Institute, Shanghai Academy of Agricultural Sciences, 2901 Beidi Road, Minhang District, Shanghai 201106, Peoples' Republic of China

²Plant Science Department, Rothamsted Research, Harpenden, Hertfordshire AL5 2JQ, United Kingdom

³Computational and Analytical Sciences Department, Rothamsted Research, Harpenden, Hertfordshire AL5 2JQ, United Kingdom

⁴Department of Computer Science, Brandenburg Technical University Cottbus-Senftenberg, Cottbus, Germany

⁵Department of Computer Science, College of Engineering, Design and Physical Sciences, Brunel University London, Uxbridge, Middlesex UB8 3PH, UK

**Correspondence: Nigel G. Halford, E-mail: nigel.halford@rothamsted.ac.uk; Jianhua Huang, E-mail: jianhua300@163.com*

Running title: Wheat asparagine synthetases

Word count: 7531

1 **ABSTRACT**

2 Asparagine synthetase activity in cereals has become an important issue with the discovery that
3 free asparagine concentration determines the potential for formation of acrylamide, a probably
4 carcinogenic processing contaminant, in baked cereal products. Asparagine synthetase
5 catalyses the ATP-dependent transfer of the amino group of glutamine to a molecule of
6 aspartate to generate glutamate and asparagine. Here, asparagine synthetase-encoding
7 polymerase chain reaction products were amplified from wheat (*Triticum aestivum*) cv. Spark
8 cDNA. The encoded proteins were assigned the names TaASN1, TaASN2 and TaASN3 on the
9 basis of comparisons with other wheat and cereal asparagine synthetases. Although very
10 similar to each other they differed slightly in size, with molecular masses of 65.49, 65.06 and
11 66.24 kDa, respectively. Chromosomal positions and scaffold references were established for
12 *TaASN1*, *TaASN2* and *TaASN3*, and a fourth, more recently identified gene, *TaASN4*. *TaASN1*,
13 *TaASN2* and *TaASN4* were all found to be single copy genes, located on Chromosomes 5, 3
14 and 4, respectively, of each genome (A, B and D), although variety Chinese Spring lacked a
15 *TaASN2* gene in the B genome. Two copies of *TaASN3* were found on Chromosome 1 of each
16 genome, and these were given the names *TaASN3.1* and *TaASN3.2*. The TaASN1, TaASN2
17 and TaASN3 PCR products were heterologously-expressed in *Escherichia coli* (TaASN4 was
18 not investigated in this part of the study). Western blot analysis identified two monoclonal
19 antibodies that recognised the three proteins, but did not distinguish between them, despite
20 being raised to epitopes SKKPRMIEVAAP and GGSNKPGVMNTV in the variable C-
21 terminal regions of the proteins. The heterologously-expressed TaASN1 and TaASN2 proteins
22 were found to be active asparagine synthetases, producing asparagine and glutamate from
23 glutamine and aspartate. The asparagine synthetase reaction was modelled using SNOOPY®
24 software and information from the BRENDA database to generate differential equations to
25 describe the reaction stages, based on mass action kinetics. Experimental data from the
26 reactions catalysed by TaASN1 and TaASN2 were entered into the model using Copasi,
27 enabling values to be determined for kinetic parameters. Both the reaction data and the
28 modelling showed that the enzymes continued to produce glutamate even when the synthesis
29 of asparagine had ceased due to a lack of aspartate.

30
31
32
33
34

Keywords: wheat, asparagine synthetase, acrylamide, food safety, enzyme activity, mathematical modelling

35 INTRODUCTION

36
37 Asparagine is an important nitrogen storage and transport molecule in many plant species due
38 to its relatively high nitrogen to carbon ratio (2:4, compared with 2:5 for glutamine, 1:5 for
39 glutamic acid and 1:4 for aspartic acid, for example) and its relative chemical inertia (Lea *et*
40 *al.*, 2007). It accumulates in its free (non-protein) form in response to a range of abiotic and
41 biotic stresses, as well as during normal physiological processes such as seed germination (Lea
42 *et al.*, 2007). In wheat grain it accumulates to very high levels in response to sulphur deficiency
43 (Muttucumaru *et al.*, 2006; Granvogl *et al.*, 2007; Curtis *et al.*, 2009; 2018) and poor disease
44 control (Curtis *et al.* 2016). There are also large differences in the free asparagine
45 concentration of grain from different wheat varieties (Curtis *et al.*, 2018). Understanding the
46 mechanisms that control free asparagine accumulation is important for improving crop yield
47 and stress resistance. However, more pressingly, it also has implications for food safety
48 because free asparagine is a precursor for acrylamide formation (reviewed by Curtis *et al.*,
49 2014; Halford *et al.*, 2012).

50
51 Acrylamide is a processing contaminant that forms during high-temperature cooking and
52 processing, particularly as a result of frying, roasting and baking. It is classed as a probable
53 (Group 2a) carcinogen by the International Agency for Research on Cancer (1994) and has
54 reproductive and neurotoxicological effects at high doses (Friedman, 2003). The European
55 Food Safety Authority (EFSA) Expert Panel on Contaminants in the Food Chain (CONTAM)
56 stated in its 2015 report that the margins of exposure for acrylamide indicate a concern for
57 neoplastic effects (EFSA Panel on Contaminants in the Food Chain (CONTAM), 2015). The
58 European Commission issued 'Indicative Values' for the presence of acrylamide in food in
59 2011, based on results reported to EFSA (European Food Safety Authority, 2011), and reduced
60 them for many product types in 2013 (European Commission, 2013). If a product is found to
61 exceed the Indicative Value, the relevant food safety authority should take action to ensure that
62 the manufacturer addresses the problem. Furthermore, the European Commission has just
63 approved strengthened risk management measures including compulsory Codes of Practice and
64 the renaming of Indicative Values as Benchmark Levels, with reduced Benchmark Levels for
65 many products (European Commission, 2017). The proposals also include a specific reference
66 to the setting of mandatory Maximum Levels for acrylamide in certain foods, stating that this
67 should be considered following the adoption of the new regulations. The proposals will come
68 before the European Parliament and European Council in 2017 and could be in force by early
69 2018.

70
71 The predominant route for the formation of acrylamide is *via* a Strecker-type degradation of
72 free asparagine by highly reactive carbonyl compounds produced within the Maillard reaction
73 (Mottram *et al.*, 2002; Stadler *et al.*, 2002; Zyzak *et al.*, 2003), and free asparagine
74 concentration is the main determinant of acrylamide-forming potential in cereal grains
75 (Muttucumaru *et al.*, 2006; Granvogl *et al.*, 2007; Curtis *et al.*, 2009; 2010; Postles *et al.*, 2013).
76 This has re-invigorated interest in the enzymes involved in asparagine synthesis and
77 breakdown, and other metabolic pathways that could impact on free asparagine concentrations.
78 Asparagine synthesis is catalysed by the enzyme asparagine synthetase, and occurs by the ATP-
79 dependent transfer of the amino group of glutamine to a molecule of aspartate to generate
80 glutamate and asparagine, and. Two asparagine synthetase genes were cloned from wheat
81 (*Triticum aestivum*) by Wang *et al.* (2005) and called *TaASN1* and *TaASN2*. *TaASN1*
82 expression in seedlings was shown to be up-regulated by treatment with abscisic acid (ABA),
83 and by salt and osmotic stress (Wang *et al.* 2005). Subsequently, its expression in leaves was
84 shown to be induced by sulphur deficiency, but to be greatly reduced when a general control

85 non-derepressible-2-type protein kinase, TaGCN2, was over-expressed (Byrne *et al.*, 2012). In
86 2016, two additional genes, *TaASN3* and *TaASN4*, were identified (Gao *et al.*, 2016), although
87 *TaASN4* was only discovered from wheat genome data and has not yet been cloned or
88 characterized. The expression of *TaASN1-3* was studied in different tissues and in response to
89 nutrition (Gao *et al.*, 2016). Notably, the expression of *TaASN2* in the embryo and endosperm
90 during mid to late grain development was shown to be the highest of any of the genes in any
91 tissue, although *TaASN1* was most responsive to sulphur supply.

92
93 Maize (*Zea mays*) and barley (*Hordeum vulgare*) also have four differentially-expressed
94 asparagine synthetase genes (Todd *et al.*, 2008; Avila-Ospina *et al.*, 2015), suggesting that this
95 is typical of the cereals. However, a full picture of the role of the different asparagine
96 synthetases will only emerge when the kinetic parameters of the enzymes have been measured.
97 This is problematic because asparagine synthetase activity in plant tissues is difficult to purify
98 and measure (Joy *et al.*, 1983; Snapp and Vance, 1986; Kudiyarova *et al.*, 2013), probably
99 because of the presence of asparaginase activities and natural inhibitors (Rognes, 1980). There
100 has also been a scarcity of antibodies for immunological analysis of purified or expressed
101 proteins. However, the enzymes encoded by three of the maize genes have been analysed after
102 heterologous expression in *Escherichia coli* and been shown to have significant differences in
103 kinetic properties (Duff *et al.*, 2011). The aim of this study was to characterize the wheat
104 asparagine synthetase gene family and to compare the enzymes encoded by *TaASN1* and
105 *TaASN2*, the two genes that are most highly expressed in the grain.

106 107 108 **MATERIALS AND METHODS**

109 110 **PLANT MATERIALS AND GROWTH CONDITIONS**

111
112 Wheat (*Triticum aestivum*) cv. Spark seeds were surface-sterilised as described by Gao *et al.*
113 (2016), and germinated in a growth room in small containers. After 7 days, seedlings were
114 harvested, flash frozen in liquid nitrogen, and then stored at -80 °C ready for use.

115 116 **MOLECULAR CLONING OF *TaASN1*, *TaASN2* AND *TaASN3***

117
118 RNA was extracted using the hot phenol method (Verwoerd *et al.*, 1989), with some
119 modification, as described previously (Postles *et al.*, 2016). It was used as a template for first-
120 strand cDNA synthesis using SuperScriptIII[®] first-strand synthesis supermix (Invitrogen,
121 supplied by Thermo Fisher Scientific, Hemel Hempstead, UK). The full-length coding
122 sequences of *TaASN1*, *TaASN2* and *TaASN3* were then amplified by polymerase chain reaction
123 (PCR). ‘Forward’ and ‘reverse’ primers for *TaASN1* were 5’-
124 ccggaattcATGTGCGGCATACTGGC and 5’-ccgctcgagAACTCTCAATTGCGACACCAG
125 (lower case letters denote additional nucleotides that were added to incorporate *EcoRI* and *XhoI*
126 restriction sites at either end of the PCR product). ‘Forward’ and ‘reverse’ primers for *TaASN2*
127 were 5’-ccggaattcATGTGCGGCATACTAGCGGTG and 5’-
128 ccgctcgagAAGTCTCAATGGCAAC, while for *TaASN3* they were 5’-
129 ccggaattcATGTGCGGCATCCTCGC and 5’-
130 ataagaatgcggccgcAAACAGCAGCTGCTGGAACA. The additional nucleotides on the
131 ‘reverse’ primer for *TaASN3* incorporated a *NotI* restriction site.

132
133 All products were amplified using Phusion[®] High-Fidelity DNA polymerase (New England
134 Biolabs, Hitchin, UK). The cycling conditions were: 30 s denaturation at 98 °C, followed by 35

135 cycles of 10 s at 98 °C, 30 s at 63 °C and 30 s at 72 °C, with a final extension period at 72 °C for
136 10 min. The resulting PCR products were purified using the Wizard PCR Clean-up system
137 (Promega, Southampton, UK) and ligated into the pGEM-T Easy Vector (Promega,
138 Southampton, UK) using the restriction sites incorporated during the PCR. Nucleotide
139 sequence analysis was performed by MWG Biotech (Wolverhampton, UK) and contigs were
140 assembled using ContigExpress or Geneious Version 8 (<http://www.geneious.com>; Kearse *et*
141 *al.*, 2012). Amino acid sequence alignments were also performed using Geneious Version 8.

142

143 GENOMIC ANALYSIS

144

145 DeCypher Tera-BLASTN Search Nucleic Query *vs.* Nucleic Database was used to assess the
146 wheat asparagine synthetase gene sequences. The NR_Gene_v0.4 scaffold wheat genome was
147 used as the database of choice (PLANT_T.aestivum_NRgene_v0.4_scaf,
148 <http://decypher1.rothamsted.ac.uk/decypher/cgi-bin/docfilter?file=/decypher/userindex.html>),
149 and the cDNA nucleotide sequences for *TaASN1* (GenBank BT009245), *TaASN2* (GenBank
150 BT009049), and *TaASN3* (GenBank AK333183) were used as the query sequences.

151

152 The returned scaffolds were downloaded and aligned to the cDNAs using the Geneious Version
153 8 software package (pairwise alignment was run using the Geneious Alignment algorithm on
154 its default settings; multiple alignments were run using the Consensus Align algorithm, again
155 on its default settings). The aligned consensus sequences were then used to search the *Triticum*
156 *aestivum* TGACv1 (Genomic sequence) database
157 ([http://plants.ensembl.org/Triticum_aestivum/Tools/Blast?db=core;tl=Igru1o47ao3Q1dXo-](http://plants.ensembl.org/Triticum_aestivum/Tools/Blast?db=core;tl=Igru1o47ao3Q1dXo-13756266)
158 [13756266](http://plants.ensembl.org/Triticum_aestivum/Tools/Blast?db=core;tl=Igru1o47ao3Q1dXo-13756266)) to assess chromosomal positioning. The returned genes from the TGAC database
159 were then re-aligned to the original cDNA sequences to confirm gene identity.

160

161 *TaASN4* was identified through its divergence from the other wheat asparagine synthetase
162 sequences. The TGAC sequence was confirmed through re-alignments to both the TGAC and
163 NR-Gene databases. BLAST searches using the PLANT_T.aestivum_nt_w7984 database were
164 used to further confirm gene identity.

165

166

167 HETEROLOGOUS EXPRESSION OF *TaASN1*, *TaASN2* AND *TaASN3* IN 168 *ESCHERICHIA COLI* (*E. COLI*)

169

170 The PCR products were excised from the PGEM[®]-T vector and ligated into the specialist
171 expression vector, pET-30a (Novagen, UK) to produce plasmids pET-30a-TaASN1, pET-30a-
172 TaASN2 and pET-30a-TaASN3. These were maintained in *E. coli* NovaBlue cells (Novagen,
173 UK), which carry *recA* and *endA* mutations, and transferred to RosettaBlue[™] cells (Novagen,
174 UK) for high levels of expression of the ASN1-3 proteins. Single colonies of the cells carrying
175 the plasmids were inoculated into medium containing 15 µg/mL kanamycin and 34 µg/mL
176 chloramphenicol. The bacteria were grown at 37 °C with shaking until they had reached mid-
177 log phase (OD 600 between 0.6 and 1.0). The culture was then split between two flasks, and
178 isopropyl β-D-1-thiogalactopyranoside (IPTG) was added to one of the flasks to a final
179 concentration of 1 mM in order to induce expression of the asparagine synthetase gene carried
180 by the plasmid. The other flask acted as an ‘un-induced’ control. The bacteria were incubated
181 with shaking at 27 °C for a further 3 h, then harvested by centrifugation and stored at -80 °C
182 until further use.

183

184 The use of the pET30a plasmid meant that the asparagine synthetase proteins were synthesized
185 with a six-residue histidine N-terminal tag, and could therefore be extracted and purified using
186 the nickel-nitrilotriacetic acid (Ni-NTA) purification system (Invitrogen, supplied by Thermo
187 Fisher Scientific, Hemel Hempstead, UK). Bacterial cells were pelleted and lysed. Proteins in
188 inclusion bodies were solubilized using NuPAGE[®] LDS-sample buffer and NuPAGE[®] Sample
189 Reducing Agent and the proteins were separated on 4-12 % Bis-Tris gels (Invitrogen, supplied
190 by Thermo Fisher Scientific, Hemel Hempstead, UK). Protein concentration was assayed using
191 a Bicinchoninic Acid Kit (Sigma-Aldrich, Gillingham, UK).

192

193 WESTERN ANALYSIS

194

195 Monoclonal antibodies were produced by Abmart (Shanghai, China). Peptides were
196 synthesized corresponding to probable epitopes in the C-terminal region of the TaASN1,
197 TaASN2 and TaASN3 proteins where the amino acid sequences show less similarity with each
198 other. Antibodies were raised to four different peptides for each of the three proteins. For
199 western analysis, soluble proteins were separated by electrophoresis on NuPAGE[®] Novex[®] 4-
200 12 % Bis-Tris gels and transferred to polyvinylidene fluoride (PVDF) membranes (13 cm × 8
201 cm) using the iBlot[®] Gel Transfer Device (Invitrogen, supplied by Thermo Fisher Scientific,
202 Hemel Hempstead, UK). Immunodetection was performed with the antibody in a 1:1000
203 dilution for 2 h at room temperature, after which the membrane was incubated for 1 h at room
204 temperature with 1:15000 horseradish peroxidase-conjugated goat anti-mouse IgG (Invitrogen,
205 supplied by Thermo Fisher Scientific, Hemel Hempstead, UK). Bands representing proteins
206 that had reacted with the anti-asparagine synthetase antibody were visualised with ECL[™]
207 Western Blotting Detection Reagents (GE Healthcare, Amersham, UK), and signals were
208 quantified by scanning densitometry using Quantity One software (Bio-Rad Laboratories,
209 Hemel Hempstead, UK).

210

211 ASPARAGINE SYNTHETASE ACTIVITY ASSAY

212

213 Purified asparagine synthetase proteins, TaASN1 and TaASN2, were added to an assay buffer
214 of 100 mM HEPES (pH 7.6), 1.6 mM aspartate, 10 mM glutamine, 10 mM ATP, 10 mM MgCl₂
215 and 1 mM DTT and incubated at 30 °C. Aliquots (100 μL) were removed after 1.5 min, 2.5
216 min, 3.5 min, 5 min, 15 min, 25 min and 35 min, placed in a 96-well filter plate and mixed with
217 100 μL of 10 % trichloroacetic acid to stop the reaction (Todd *et al.*, 2008; Duff *et al.*, 2011;
218 Kudiyarova *et al.*, 2013). Two replicate assays were done.

219

220 The free asparagine and glutamate produced in the reaction was detected after derivatisation
221 with o-phthalaldehyde reagent (Sigma-Aldrich, Gillingham, UK). The fluorescent derivative
222 was measured by high performance liquid chromatography (HPLC) using a Waters Alliance
223 2795 HPLC system fitted with a Waters 474 Scanning Fluorescence Detector (Waters, Elstree,
224 UK). A Symmetry C₁₈, 4.6 × 150 mm column (for particle size 3.5 μm to 5 μm) (Waters,
225 Elstree, UK) was used, and the fluorescence detector was set with an excitation wavelength of
226 340 nm and emission wavelength of 455 nm. For calibration, standards were used to provide
227 areas under the HPLC peaks corresponding to asparagine and glutamate concentrations of 0, 5,
228 10, 15 and 20 nmol. The areas were modelled on the concentrations using linear regression, so
229 that, by inverting the resulting linear equation, estimated concentrations of the amino acids and
230 the asparagine synthetase enzyme could be made given HPLC areas for the sample aliquots
231 taken at the seven sampling time points. Standards were run separately for each experiment.

232

233

234 **MODELLING THE ASPARAGINE SYNTHETASE REACTION**

235

236 A model for the reactions catalysed by asparagine synthetases TaASN1 and TaASN2 was
237 constructed using the SNOOPY[®] tool ([http://www-dssz.informatik.tu-](http://www-dssz.informatik.tu-cottbus.de/DSSZ/Software/)
238 [cottbus.de/DSSZ/Software/](http://www-dssz.informatik.tu-cottbus.de/DSSZ/Software/)) (Heiner *et al.*, 2012) for designing, animating and simulating Petri
239 Nets. The model was then exported to Copasi 4.16 (Build 104) (Hoops *et al.*, 2006). Data for
240 the reaction parameters were taken from the Brenda enzyme database ([http://www.brenda-](http://www.brenda-enzymes.org/)
241 [enzymes.org/](http://www.brenda-enzymes.org/)).

242

243

244 **RESULTS**

245

246 **MOLECULAR CLONING AND IDENTIFICATION OF THREE ASPARAGINE** 247 **SYNTHETASE-ENCODING cDNAS FROM WHEAT (*TRITICUM AESTIVUM*)**

248

249 Gao *et al.* (2016) identified three distinct asparagine synthetase gene nucleotide sequences in
250 the GenBank database: *TaASN1* (Wang *et al.*, 2005; GenBank AY621539; BT009245),
251 *TaASN2* (GenBank BT009049) and *TaASN3* (GenBank AK333183). *TaASN1* and *TaASN2*
252 were already annotated as asparagine synthetases, but the *TaASN3* entry had not been up to that
253 point. Gao *et al.* also identified a fourth gene, *TaASN4*, from a BLAST search of wheat genome
254 data (www.cerealsdb.uk.net; Wilkinson *et al.*, 2012). *TaASN4* is present in cultivated and wild
255 rice (*Oryza sativa* and *Oryza brachyantha*), *B. distachyon*, *Ae. tauschii*, foxtail millet (*Setaria*
256 *italica*) and maize (*Zea mays*), as well as wheat (Gao *et al.*, 2016), but to date has not been
257 cloned from or characterized in wheat.

258

259 Gao *et al.* (2016) described the differential expression of *TaASN1*, *TaASN2* and *TaASN3* in
260 different wheat tissues and in response to nitrogen and sulphur feeding, with expression of
261 *TaASN2* in the embryo and to a lesser extent the endosperm of the grain during mid-
262 development being far higher than the expression of any of the genes in any other tissue,
263 although *TaASN1* showed most response to nutrition. This suggests that *TaASN2* expression
264 in the grain is the primary determinant of asparagine levels, either for protein synthesis or
265 accumulation in the free form, rather than import of free asparagine from other tissues, at least
266 under normal (nutrient-sufficient) conditions, making *TaASN2* a potential target for genetic
267 interventions to reduce free asparagine accumulation in wheat grain. However, modelling of
268 the processes controlling the accumulation of free asparagine in order to confirm this requires
269 information on the kinetic parameters of asparagine synthetase enzymes to add to the data on
270 gene expression, and this was the aim of the current study.

271

272 To that end, *TaASN1*, *TaASN2* and *TaASN3* PCR products were amplified from wheat cv. Spark
273 using primers designed from published sequences (see Materials and Methods Section).
274 *TaASN1* from this variety was found to encode a protein of 585 amino acid residues with a
275 molecular weight of 65.49 kDa, while *TaASN2* encoded a slightly smaller protein of 581
276 residues, molecular weight 65.06 kDa, and *TaASN3* a slightly larger protein of 591 residues,
277 molecular weight 66.24 kDa. The nucleotide sequences have been deposited in the GenBank
278 database and been given accession numbers KY937995, KY937996 and KY937997.
279 Comparisons of the derived amino acid sequences of the proteins with those encoded by the
280 nucleotide sequences already in the database confirmed that the three PCR products were
281 derived from *TaASN1*, *TaASN2* and *TaASN3* (Table 1).

282

283 The amino acid sequences of the three proteins are aligned in Figure 1. All three share
284 conserved amino acid residues typical of asparagine synthetases (highlighted in red in Figure
285 1), including the essential residues of a *purF*-type glutamine-binding site, Cys², Asp³⁴ and
286 His¹⁰⁴ (Mei and Zalkin, 1989), and other residues important for glutamine binding and
287 positioning that have been identified from the *E. coli* AsnB enzyme (Arg⁵⁰, Leu⁵¹, Ile⁵³, Asn⁷⁵,
288 Gly⁷⁶, Glu⁷⁷ and Asp⁹⁸) (Larsen *et al.*,1999). Residues Thr³¹⁶, Thr³¹⁷, Arg³¹⁹ and Cys⁵²³ are
289 involved in the binding of aspartate and ATP (Boehlein *et al.*, 1994a; 1994b; 1997a; 1997b),
290 while Leu²³¹, Val²⁶⁷, Ser³⁴¹ and Gly³⁴² have been recognized as the anchoring points for the
291 AMP moiety (Larsen *et al.*,1999). Interestingly, Val²⁶⁷ is replaced with a different hydrophobic
292 residue, Ile, in TaASN3. Lastly, the Ser, Gly, Gly, Leu, Asp, Ser motif beginning at position
293 233 is conserved in all of the asparagine synthetases characterized to date and may be involved
294 in pyrophosphate binding (Richards and Schuster, 1998).

295

296 GENE STRUCTURE AND LOCATION

297

298 BLAST searches were performed of the wheat (*Triticum aestivum*) scaffold genome in the non-
299 redundant genome database (NR_Gene_v0.4) using the cDNA sequences for *TaASN1*, *TaASN2*
300 and *TaASN3* (Gao *et al.*, 2016). This search also identified scaffolds for *TaASN4*, which to date
301 has not been cloned from bread wheat (Gao *et al.*, 2016). The returned scaffolds were aligned
302 to the cDNAs to identify exons and introns, and the results confirmed by searches of the
303 *Triticum aestivum* TGACv1 genomic sequence. The consensus sequences derived from these
304 alignments were then used to search the Ensembl wheat database to determine the
305 chromosomal positioning of the genes. Note that both the NR and TGAC genome data are from
306 variety Chinese Spring.

307

308 The chromosomal positions and scaffold references for the genes are given in Table 2. *TaASN1*,
309 *TaASN2* and *TaASN4* were all found to be single copy genes, located on Chromosomes 5, 3
310 and 4, respectively, of each genome (A, B and D), except that *TaASN2* was not present in the
311 B genome. Analysis of unpublished wheat genome data (Alison Huttly, Rothamsted Research,
312 personal communication) suggests that not all wheat varieties lack a *TaASN2* gene on
313 Chromosome 3B, but the relative prevalence of the presence or absence of a B genome *TaASN2*
314 gene cannot yet be assessed. In the case of *TaASN3*, there were two copies on Chromosome 1
315 of each genome, and these were given the names *TaASN3.1* and *TaASN3.2*.

316

317 The structures of the genes are shown in Figure 2, illustrating the considerable divergence of
318 intron/exon patterns between the different genes, but conservation of structure within each
319 group of homeologues. The three *TaASN1* homeologues, on Chromosomes 5A, B and D, are
320 the shortest at approximately 3 kb from the ATG translation start codon to the translation stop
321 codon, including 12 exons. The two *TaASN2* homeologues are approximately 4 kb in length,
322 with 11 exons, and the three *TaASN3.1* and *TaASN3.2* homeologues just over and just under 6
323 kb, respectively, making them the longest group. The two *TaASN3* genes share a similar
324 intron/exon pattern, with 15 exons. The three *TaASN4* homeologues are just under 4 kb in
325 length, with 12 exons, except that the *TaASN4* gene on Chromosome 4B lacks exon 8. Clearly,
326 this deletion may affect the activity of the enzyme encoded by the gene.

327

328

329 HETEROLOGOUS EXPRESSION AND PURIFICATION OF TaASN1, TaASN2 and 330 TaASN3

331

332 The TaASN1, TaASN2 and TaASN3 PCR products were sub-cloned into vector pET-30a and

333 the resulting plasmids transformed into *E. coli* Rosetta DE3 cells to enable expression of the
334 asparagine synthetase proteins. Use of this system meant that the proteins were synthesized
335 with a six-residue histidine 'tag', enabling them to be purified on a Ni-NTA agarose column.
336 Expression of the proteins was induced by addition of IPTG to the cell culture medium.

337
338 The result of SDS-polyacrylamide gel electrophoresis (SDS-PAGE) of the expressed TaASN1,
339 TaASN2 and TaASN3 proteins in both crude *E. coli* lysates and after purification on the
340 column is shown in Figure 3. The proteins were solubilized by addition of NuPAGE[®] LDS-
341 sample buffer, which contains lithium dodecyl sulphate at a pH of 8.4, and NuPAGE[®] Sample
342 Reducing Agent, which contains dithiothreitol. An un-induced control is also shown (Figure
343 3) for each protein. The result showed the TaASN proteins to be highly expressed and readily
344 purified.

345
346

347 **WESTERN ANALYSIS; SCREENING OF PANEL OF ANTIBODIES**

348

349 A panel of monoclonal antibodies was raised to peptides (Table 3) corresponding to epitopes
350 within the variable C-terminal regions of the proteins (Figure 1) with the aim of identifying
351 antibodies that showed high specificity for the TaASN proteins and could distinguish between
352 them. A western blot of the heterologously-expressed TaASN1 proteins reacted with
353 antibodies raised to two of the peptides, SKKPRMIEVAAP and GGSNKPGVMNTV, is
354 shown in Figure 4. These two antibodies showed the highest specificity for the TaASN
355 proteins, with the least non-specific binding, although all of the antibodies reacted with the
356 TaASN proteins (not shown). However, none of the antibodies distinguished between the three
357 asparagine synthetases. This was surprising because of the divergence of the amino acid
358 sequences in this region (Figure 1). The SKKPRMIEVAAP epitope is present in TaASN1,
359 while the GGSNKPGVMNTV epitope is at almost the same position in TaASN2 (indicated
360 with a blue box in Figure 1). In each case there are only four identical residues and two
361 conservative substitutions between the two proteins, and the similarity with TaASN3 is even
362 lower. Nevertheless, TaASN1, TaASN2 and TaASN3 could be distinguished on the basis of
363 size, with TaASN2 (65.06 kDa) migrating the furthest in the SDS-PAGE, followed by TaASN1
364 (65.49 kDa) and TaASN3 (66.24 kDa) (Figure 4).

365
366

367 **PRODUCTION OF ASPARAGINE AND GLUTAMATE IN REACTIONS** 368 **CATALYSED BY ASPARAGINE SYNTHETASES, TaASN1 and TaASN2**

369

370 The production of asparagine and glutamate from aspartate and glutamine by TaASN1 and
371 TaASN2 was measured in standard assays adapted from those described by Todd *et al.* (2008),
372 Duff *et al.* (2011) and Kudiyarova *et al.* (2013). The reactions were sampled at 0, 1.5, 2.5, 3.5,
373 5, 15, 25 and 35 minutes and the asparagine and glutamate produced in the reaction were
374 detected after conversion to a fluorescent derivative using o-phthalaldehyde reagent, separation
375 by HPLC and detection of the fluorescent derivative with a scanning fluorescence detector. All
376 three enzymes produced asparagine and glutamate, confirming that all three were asparagine
377 synthetases. The concentrations measured for the reactions are given in Supplementary File S1
378 for the two replicate assays done. Data from the calibration of the HPLC areas using standard
379 concentrations of asparagine and glutamate are also given. The results up to the 15 minute
380 time point, by which time the concentrations of both asparagine and glutamate had plateaued,
381 are shown graphically in Figure 5.

382

383 It was clear that the reactions catalysed by both asparagine synthetases proceeded much more
384 rapidly than had been reported for heterologously-expressed maize or soybean enzymes (Todd
385 *et al.*, 2008; Duff *et al.*, 2014). The reaction buffer contained 1.6 mM aspartate and 10 mM
386 glutamine, meaning that glutamine was present in relative excess compared with aspartate. In
387 both cases, the concentration of glutamate increased at a faster rate than the concentration of
388 asparagine (Figure 5). By the 5 minute timepoint in both reactions, the concentrations of both
389 products were at or close to their maximum, indicating that the concentration of the reactants
390 had become depleted. Notably, at this point, the concentration of glutamate was more than
391 double that of asparagine, and the measured concentration of asparagine was actually slightly
392 higher than would be expected given the starting concentration of aspartate.

393

394

395 MODELLING THE ASPARAGINE SYNTHETASE REACTION

396

397 The SNOOPY[®] tool was used to construct a continuous Petri net model which incorporates
398 underlying ordinary differential equations (ODEs), representing the reaction catalysed by
399 asparagine synthetases, TaASN1 and TaASN2. The model was based on the reaction stages
400 proposed by Gaufichon *et al.* (2010), with some modifications, and the experimental data,
401 assuming mass action kinetics. A schematic diagram of the model is given in Figure 6. It
402 comprises metabolites ('places' in Petri Net terminology) indicated by circles, and reactions
403 ('transitions') indicated by squares, connected by arrows ('edges'). The concentration of
404 metabolites is represented abstractly by numbers on places. The model comprises one
405 compartment (cell) with eleven molecules (species): adenosine monophosphate (AMP),
406 asparagine (Asn), asparagine synthetase enzyme (for the purpose of the modelling annotated
407 as ASNe), asparagine synthetase enzyme complexed with glutamine (ASNe-Gln), asparagine
408 synthetase enzyme complexed with ammonia (ASNe-NH₃), aspartate (Asp), adenosine
409 triphosphate (ATP), β-aspartyl-complex (βAsp-AMP-ASNe-NH₃), glutamine (Gln), glutamate
410 (Glu) and magnesium ions (Mg²⁺). The four elementary biochemical reactions involved in the
411 formation of asparagine are represented by the following equations:

412

413 • Reaction r1: ASNe + Gln → ASNe-Gln

414

415 • Reaction r2: ASNe-Gln → Glu + ASNe-NH₃

416

417 • Reaction r3: ASNe-NH₃ + Asp + ATP + Mg²⁺ (+ H₂O) → βAsp-AMP-ASNe-NH₃ + Mg²⁺
418 (+ PPi)

419

420 • Reaction r4: βAsp-AMP-ASNe-NH₃ → Asn + ASNe + AMP

421

422 Note that H₂O and PPi (pyrophosphate, P₂O₇⁴⁻) are in parentheses because they are ubiquitous
423 and therefore were not included in the model. The behaviour of each reaction is dependent on
424 the corresponding parameter values and the initial concentrations of the metabolites. The model
425 additionally includes a dissociation step for the ASNe-NH₃ complex (reaction 'D' highlighted
426 in red in Figure 6), because this better fits the observed experimental data: Reaction D: ASNe-
427 NH₃ → ASNe

428

429 The following ordinary differential equations were generated by the SNOOPY[®] Petri Net
430 software (up to some naming adaptations to comply with the software requirements) to describe
431 the mass action reactions determining the behaviour of the eleven metabolites in the model:

432

$$433 \quad d \text{Gln}/dt = - (k1 * \text{Gln} * \text{ASNe}) \quad (1)$$

434

$$435 \quad d \text{ASNe-Gln}/dt = (k1 * \text{Gln} * \text{ASNe}) - (k2 * \text{ASNe-Gln}) \quad (2)$$

436

$$437 \quad d \text{ASNe}/dt = (k4 * \beta \text{Asp-AMP-ASNe-NH}_3) + (kD * \text{ASNe-NH}_3) - (k1 * \text{Gln} * \text{ASNe}) \quad (3)$$

438

$$439 \quad d \text{Glu}/dt = (k2 * \text{ASNe-Gln}) \quad (4)$$

440

$$441 \quad d \text{ASNe-NH}_3/dt = (k2 * \text{ASNe-Gln}) - (k3 * \text{ASNe-NH}_3 * \text{Asp} * \text{Mg}^{2+} * \text{ATP}) - (kD * \text{ASNe-NH}_3) \quad (5)$$

442

$$443 \quad d \text{Asp}/dt = - (k3 * \text{ASNe-NH}_3 * \text{Asp} * \text{Mg}^{2+} * \text{ATP}) \quad (6)$$

444

$$446 \quad d \beta \text{Asp-AMP-ASNe-NH}_3/dt = (k3 * \text{ASNe-NH}_3 * \text{Asp} * \text{Mg}^{2+} * \text{ATP}) - (k4 * \beta \text{Asp-AMP-ASNe-NH}_3) \quad (7)$$

447

$$448 \quad d \text{Asn}/dt = (k4 * \beta \text{Asp-AMP-ASNe-NH}_3) \quad (8)$$

449

$$451 \quad d \text{AMP}/dt = (k4 * \beta \text{Asp-AMP-ASNe-NH}_3) \quad (9)$$

452

$$453 \quad d \text{ATP}/dt = 0 \quad (10)$$

454

$$455 \quad d \text{Mg}^{2+}/dt = 0 \quad (11)$$

456

457

458 The model structure and corresponding induced behaviour indicates that: (a) asparagine
 459 synthesis is dependent on the aspartic acid (aspartate), glutamine and ATP concentration; (b)
 460 when aspartic acid is depleted but glutamine is still available, asparagine synthetase will
 461 continue to hydrolyse glutamine to glutamic acid, which is consistent with the observed
 462 experimental data (Figure 5); (c) if all substrates are available except for ATP (i.e. ATP would
 463 only be an input to the system, unlike in the current model), the limiting factor becomes ATP.

464

465 The parameters (Table 4) were determined using the parameter estimation function of Copasi
 466 (version 4.16) (Hoops et al. 2006) based on the Hooke and Jeeves (1961) method. The values
 467 for the TaASN1 enzyme were defined using the following concentrations (mg/mL): ASNe
 468 between 1e-06 and 1e+06 with start value = 0.1; Glu between 1e-06 and 1e+06 with start value
 469 = 0.0; Asn between 1e-06 and 1e+06 with start value = 0.0, based on the data for Glu, Asn and
 470 ASNe provided in Supplementary File S1. The values for TaASN2 were the same, except for
 471 the start value of ASNe which was set at 0.09. The parameter estimation tasks were run for
 472 both enzymes for 2100 seconds with 2000 steps, size 1.05, with resulting rate values in units
 473 of mg/mL/s. The corresponding plots showing the time-series simulation results from the
 474 parameter fitting against the experimental data are given in Figure 7 for TaASN1 and Figure 8
 475 for TaASN2, using initial concentrations of TaASN1 = 2.03 nmol/mL and TaASN2 = 2.10
 476 nmol/mL.

477

478

479 DISCUSSION

480

481 Wheat is now known to contain four classes of asparagine synthetase genes, *TaASN1-4* (Gao
 482 et al., 2016). Our study established that there are single copies of *TaASN1*, *TaASN2* and

483 *TaASN4*, and two of *TaASN3*, and identified their chromosomal locations. The relatively simple
484 structure of the gene family means that genetic interventions to reduce free asparagine
485 accumulation and thereby acrylamide-forming potential in wheat grain are more likely to be
486 successful. The antibodies raised in the study would be useful tools in the analysis of plants in
487 which asparagine synthetase gene expression has been modified. The antibodies did not
488 distinguish between *TaASN1*, *TaASN2* and *TaASN3*, but it was possible to separate the
489 enzymes on SDS-PAGE due to their slightly different sizes.

490

491 The study also showed that wheat asparagine synthetase enzymes, *TaASN1* and *TaASN2*, can
492 be expressed in *E. Coli* and analysed biochemically. Wheat asparagine synthetase activity has
493 been measured before (Kudiyarova *et al.*, 2013) but this was in plant extracts, so the results
494 were not directly comparable to those obtained here. However, Todd *et al.* (2008) and Duff *et al.*
495 (2014) analysed heterologously-expressed enzymes, the former from maize and the latter
496 from maize and soybean. The reactions were not modelled, because their overall activity was
497 very low, Todd *et al.* (2008) reporting a specific activity for asparagine production of 1-2
498 nmoles per min per mg of protein. The reaction buffer used by Todd *et al.* (2008) contained
499 1.6 mM aspartate and 1 mM glutamine, while Duff *et al.* (2011) used a buffer containing 1.6
500 mM aspartate and 2 mM glutamine, and the reactions were sampled over a period of 60 to 90
501 minutes. In this study, a buffer was used containing 1.6 mM aspartate and 10 mM glutamine,
502 as well as 10 mM ATP and 10 mM MgCl₂, meaning that glutamine was present in relative
503 excess compared with aspartate. The reactions catalysed by the wheat asparagine synthetases
504 proceeded much more rapidly than had been reported for the maize or soybean enzymes. By
505 the 5 minute timepoint, the concentrations of glutamate and asparagine were at or close to their
506 maximum, indicating that the concentration of the reactants had become depleted.

507

508 A continuous Petri net model based on mass-action kinetics was constructed using SNOOPY®
509 software to describe the reaction catalysed by asparagine synthetase, and a set of differential
510 equations was generated to describe each part of the reaction. It was notable from the
511 experimental data that the concentration of glutamate increased at a faster rate than the
512 concentration of asparagine. Indeed, the product concentrations for both enzymes plateaued
513 with the concentration of glutamate more than double that of asparagine, although the ratio of
514 glutamate to asparagine was higher for *TaASN1* than *TaASN2*. This indicates that the early
515 stages of the reaction (r1 and r2 in the model) can proceed faster than and independently of the
516 later stages (r3 and r4), consistent with the hypothesis proposed by Gaufichon *et al.* (2010) that
517 steps r1 to r4 occur sequentially rather than simultaneously. So, despite the overall equation of
518 the reaction being Glutamine + Aspartate + ATP → Glutamate + Asparagine + AMP + PPi,
519 glutamate synthesis can proceed independently of asparagine synthesis when aspartate is not
520 available.

521

522 Modelling of the reactions catalysed by *TaASN1* and *TaASN2* showed the two enzymes to be
523 biochemically very similar except for the rate parameter (kD) for the dissociation step (Table
524 4). The careful fitting resulted in parameter values k1 to k4 which were within expected
525 biochemical ranges (Meister, 1974). The dissociation reaction, D, which we postulate in order
526 to be able to fit the overall model to the data, is currently not described in the literature.
527 However, the higher kD value for *TaASN1* could explain the higher ratio of glutamate to
528 asparagine produced in the *TaASN1* reaction compared with the *TaASN2* reaction.

529

530 Gene expression analyses have shown *TaASN1* and *TaASN2* to be the most highly expressed
531 asparagine synthetase genes in wheat grain, with *TaASN2* expression rising to 10 times that of
532 *TaASN1* by mid-development (Gao *et al.*, 2016). Given this and the similarity in the

533 biochemical data obtained for the two asparagine synthetases in the present study, we conclude
534 that TaASN2 is the major enzyme synthesising asparagine in wheat grain, and therefore an
535 appropriate target for genetic interventions to reduce free asparagine accumulation.
536

537

538 ACKNOWLEDGEMENTS

539

540 HX and RG were supported as visiting workers at Rothamsted Research by Shanghai
541 Agriculture Applied Technology Development Program, China (Grant No.Z20160101) and
542 overseas visiting grants from Shanghai Academy of Agricultural Sciences, Shanghai, Peoples'
543 Republic of China. TYC was supported by the Biotechnology and Biological Sciences
544 Research Council (BBSRC) of the United Kingdom and a consortium of companies and
545 organisations from the wheat supply chain through stand-alone LINK project 'Genetic
546 improvement of wheat to reduce the potential for acrylamide formation during processing'.
547 NGH was supported at Rothamsted Research by the BBSRC via the 20:20 Wheat® and
548 Designing Future Wheat Programmes.
549

549

550

REFERENCES

- Avila-Ospina, L., Marmagne, A., Talbotec, J. and Krupinska, K. (2015). The identification of new cytosolic glutamine synthetase and asparagine synthetase genes in barley (*Hordeum vulgare* L.), and their expression during leaf senescence. *J. Exp. Bot.* 66, 2013-2026.
- Boehlein, S.K., Richards, N.G., Walworth, E.S. and Schuster, S.M. (1994a). Arginine 30 and asparagine 74 have functional roles in the glutamine dependent activities of *Escherichia coli* asparagine synthetase B. *J. Biol Chem.* 269, 26789-26795.
- Boehlein, S.K., Richards, N.G. and Schuster, S.M. (1994b). Glutamine-dependent nitrogen transfer in *Escherichia coli* asparagine synthetase B. Searching for the catalytic triad. *J. Biol. Chem.* 269, 7450-7457.
- Boehlein, S.K., Walworth, E.S., Richards, N.G. and Schuster, S.M. (1997a). Mutagenesis and chemical rescue indicate residues involved in beta-aspartyl-AMP formation by *Escherichia coli* asparagine synthetase B. *J. Biol. Chem.* 272, 12384-12392.
- Boehlein, S.K., Walworth, E.S. and Schuster, S.M. (1997b). Identification of cysteine-523 in the aspartate binding site of *Escherichia coli* asparagine synthetase B. *Biochemistry* 36, 10168-10177.
- Byrne, E.H., Prosser, I., Muttucumar, N., Curtis, T.Y., Wingler, A., Powers, S. and Halford, N.G. (2012). Over-expression of GCN2-type protein kinase in wheat has profound effects on free amino acid concentration and gene expression. *Plant Biotech. J.* 10, 328-340.
- Curtis, T.Y., Muttucumar, N., Shewry, P.R., Parry, M.A., Powers, S.J., Elmore, J.S., Mottram, D.S., Hook, S. and Halford, N.G. (2009). Effects of genotype and environment on free amino acid levels in wheat grain: implications for acrylamide formation during processing. *J. Agric. Food Chem.* 57, 1013-1021.
- Curtis, T.Y., Powers, S.J., Balagiannis, D., Elmore, J.S., Mottram, D.S., Parry, M.A.J., Raksegi, M., Bedő, Z., Shewry, P.R. and Halford, N.G. (2010). Free amino acids and sugars in rye grain: implications for acrylamide formation. *J. Agric. Food Chem.* 58, 1959-1969.

- Curtis, T.Y., Postles, J. and Halford, N.G. (2014). Reducing the potential for processing contaminant formation in cereal products. *J. Cer. Sci.* 59, 382-392.
- Curtis, T.Y., Powers, S.J. and Halford, N.G. (2016). Effects of fungicide treatment on free amino acid concentration and acrylamide-forming potential in wheat. *J. Agric. Food Chem.* 64, 9689-9696.
- Curtis, T.Y., Powers, S.J., Wang, R. and Halford, N.G. (2018). Effects of variety, year of cultivation and sulphur supply on the accumulation of free asparagine in the grain of commercial wheat varieties. *Food Chem.* 239, 304-313.
- Duff, S.M.G., Qi, Q., Reich, T., Wu, X., Brown, T., Crowley, J.H. and Fabbri, B. (2011). A kinetic comparison of asparagine synthetase isozymes from higher plants. *Plant Physiol. Biochem.* 49, 251-256.
- EFSA Panel on Contaminants in the Food Chain (CONTAM) (2015). Scientific opinion on acrylamide in food. *EFSA J.* 13, 4104.
- European Commission (2013). Commission recommendation of 8 November 2013 on investigations into the levels of acrylamide in food. European Commission, Brussels, Belgium.
- European Commission (2017). Establishing mitigation measures and benchmark levels for the reduction of the presence of acrylamide in food. European Commission, Brussels, Belgium.
- Friedman, M. (2003). Chemistry, *Biochem.* and safety of acrylamide. A review. *J. Agric. Food Chem.* 51, 4504-4526.
- Gao, R., Curtis, T.Y., Powers, S.J., Xu, H., Huang, J. and Halford, N.G. (2016). Food safety: Structure and expression of the asparagine synthetase gene family of wheat. *J. Cer. Sci.* 68, 122-131.
- Gaufichon, L., Reisdorf-Cren, M., Rothstein, S.J., Chardon, F. and Suzuki, A. (2010). Biological functions of asparagine synthetase in plants. *Plant Sci.* 179, 141-153.
- Granvogl, M., Wieser, H., Koehler, P., Von Tucher, S. and Schieberle, P. (2007). Influence of sulfur fertilization on the amounts of free amino acids in wheat. Correlation with baking properties as well as with 3-aminopropionamide and acrylamide generation during baking. *J. Agric. Food Chem.* 55, 4271-4277.
- Halford, N.G., Curtis, T.Y., Muttucumaru, N., Postles, J., Elmore, J.S. and Mottram, D.S., (2012). The acrylamide problem: a plant and agronomic science issue. *J. Exp. Bot.* 63, 2841-2851.
- Heiner, M., Herajy, M., Liu, F., Rohr, C. and Schwarick, M. (2012). Snoopy – a unifying Petri Net tool. In: Application and Theory of Petri Nets, Volume 7347 of the series Lecture Notes in Computer Science. Springer, Hamburg, pp. 398-407.
- Hooke, R. and Jeeves, T.A. (1961). Direct search solution of numerical and statistical problems. *J. Assoc. Comp. Machinery (ACM)* 8, 212-229.
- Hoops, S., Sahle, S., Gauges, R., Lee, C., Pahle, J., Simus, N., Singhal, M., Xu, L., Mendes, P. and Kummer, U. (2006). COPASI: a COMplex PATHway SIMulator. *Bioinformatics* 22, 3067-3074.
- International Agency for Research on Cancer (1994). Some Industrial Chemicals; IARC Monographs on the Evaluation of Carcinogenic Risks to Humans. Vol. 60. International Agency for Research on Cancer (IARC), Lyon.
- Joy, K.W., Ireland, R.J. and Lea, P.J. (1983). Asparagine synthesis in pea leaves, and the occurrence of an asparagine synthetase inhibitor. *Plant Physiol.* 73, 165-168.
- Kearse, M., Moir, R., Wilson, A., Stones-Havas, S., Cheung, M., Sturrock, S., Buxton, S., Cooper, A., Markowitz, S., Duran, C., Thierer, T., Ashton, B., Mentjies, P. and Drummond, A. (2012). Geneious Basic: an integrated and extendable desktop software

- platform for the organization and analysis of sequence data. *Bioinformatics* 28, 1647-1649.
- Kudiyarova, Zh.S., Muttucumaru, N., West, J.S. and Halford, N.G. (2013). Activity of enzymes associated with asparagine synthesis and breakdown in wheat under biotic and abiotic stress conditions. *Aspects Applied Biol.* 116, 119-124.
- Larsen, T.M., Boehlein, S.K., Schuster, S.M., Richards, N.G., Thoden, J.B. and Holden, H.M. (1999). Three-dimensional structure of *Escherichia coli* asparagine synthetase B: a short journey from substrate to product. *Biochemistry* 38, 16146-16157.
- Lea, P.J., Sodek, L., Parry, M.A., Shewry, P.R. and Halford, N.G. (2007). Asparagine in plants. *Ann. Appl. Biol.* 150, 1-26.
- Mei, B. and Zalkin, H. (1989). A cysteine-histidine-aspartate catalytic triad is involved in glutamine amide transferase function in *purf*-type glutamine amidotransferases. *J. Biol. Chem.* 264, 16613-16619.
- Meister, L. (1974). Asparagine synthesis. In: Boyer, P.D. (ed.), *The Enzymes*, Volume 10 (3rd Edition), pp. 561-580. Academic Press, New York.
- Mottram, D.S., Wedzicha, B.L. and Dodson, A.T. (2002). Acrylamide is formed in the Maillard reaction. *Nature* 419, 448-449.
- Muttucumaru, N., Halford, N.G., Elmore, J.S., Dodson, A.T., Parry, M., Shewry, P.R. and Mottram, D.S. (2006). Formation of high levels of acrylamide during the processing of flour derived from sulfate-deprived wheat. *J. Agric. Food Chem.* 54, 8951-8955.
- Postles, J., Powers, S.J., Elmore, J.S., Mottram, D.S. and Halford, N.G. (2013). Effects of variety and nutrient availability on the acrylamide forming potential of rye grain. *J. Cer. Sci.* 57, 463-470.
- Postles, J., Curtis, T.Y., Powers, S.J., Elmore, J.S., Mottram, D.S. and Halford, N.G. (2016). Changes in free amino acid concentration in rye grain in response to nitrogen and sulfur availability, and expression analysis of genes involved in asparagine metabolism. *Frontiers Plant Sci.* 7, 917.
- Richards, N.G.J. and Schuster, S.M. (1998). Mechanistic issues in asparagine synthetase catalysis. *Adv. Enzymol. Relat. Areas Molec. Biol.* 72, 145-198.
- Rognes, S.E. (1980). Anion regulation of lupine asparagine synthetase: chloride activation of the glutamine-utilizing reactions. *Phytochemistry* 19, 2287-2293.
- Snapp, S.S. and Vance, C.P. (1986). Asparagine biosynthesis in alfalfa (*Medicago sativa* L.) root nodules. *Plant Physiol.* 82, 390-395.
- Stadler, R.H., Blank, I., Varga, N., Robert, F., Hau, J., Guy, P.A., Robert, M-C. and Riediker, S. (2002). Acrylamide from Maillard reaction products. *Nature* 419, 449-450.
- Todd, J., Screen, S., Crowley, J., Penga, J., Andersen, A., Brown, T., Qi, Q., Fabri, B. and Duff, S.M.G. (2008). Identification and characterization of four distinct asparagine synthetase (*AsnS*) genes in maize (*Zea mays* L.). *Plant Sci.* 175, 799-808.
- Verwoerd, T.C., Dekker, B.M.M. and Hoekema, A. (1989). A small-scale procedure for the rapid isolation of plant RNAs. *Nucl. Acids Res.* 17, 2362.
- Wang, H., Liu, D., Sun, J. and Zhang, A. (2005). Asparagine synthetase gene *TaASN1* from wheat is up-regulated by salt stress, osmotic stress and ABA. *J. Plant Physiol.* 162, 81-89.
- Wilkinson, P.A., Winfield, M.O., Barker, G.L.A., Allen, A.M., BurrIDGE, A., Coghill, J.A. and Edwards, K.J. (2012). CerealsDB 2.0: an integrated resource for plant breeders and scientists. *BMC Bioinformatics* 13, 219.
- Zyzak, D.V., Sanders, R.A., Stojanovic, M., Tallmadge, D.H., Eberhart, B.L., Ewald, D.K., Gruber, D.C., Morsch, T.R., Strothers, M.A., Rizzi, G.P. and Villagran, M.D. (2003). Acrylamide formation mechanism in heated foods. *J. Agric. Food Chem.* 51, 4782-4787.

Conflict of interest statement

The project was supported by a number of companies and organisations from the wheat supply chain.

In review

TABLE 1. Amino acid sequence identity between the asparagine synthetases encoded by the PCR products amplified from wheat cv. Spark and wheat asparagine synthetases from the GenBank database.

	AY621539 (TaASN1)	BT009049 (TaASN2)	AK333183 (TaASN3)
Spark TaASN1	99%	88%	77%
Spark TaASN2	88%	100%	78%
Spark TaASN3	80%	78%	97%

In review

TABLE 2. Chromosomal position and scaffold references for wheat (*Triticum aestivum*) cv. Chinese Spring asparagine synthetase genes (*TaASN1-4*).
 (<http://decypher1.rothamsted.ac.uk/decypher/cgi-bin/docfilter?file=/decypher/userindex.html> and
http://plants.ensembl.org/Triticum_aestivum/Tools/Blast?db=core;tl=Igru1o47ao3Q1dXo-13756266)

Gene	Chromosomal Position	NR_gene v0.4 scaffold reference	TGACv.1 scaffold reference
<i>TaASN1</i>	5AL	10829_chr5A	376022_5AL:32188-35544
	5BL	86991_chr5B	404794_5BL:130599-132056
	5DL	24580_chr5D	438333_5DL:8628-10259
<i>TaASN2</i>	3AS	147930_chr3A	210989_3AS:73,515-78,055
	3DS	57063_chr3D	271746_3DS:53902-54460
<i>TaASN3</i>	1AL	72517_chr1A	004377_1AL:6267-12623
	1BL	94459_chr1B	032370_1BL:29616-29990
	1DL	40616_chr1D	061978_1DL:28081-28357
	1AL	81741_chr1A	002273_1AL:9143-9387
	1BL	95194_chr1B	031075_1BL:62894-63123
	1DL	86160_chr1D	061247_1DL:39750-39978
<i>TaASN4</i>	4AS	103865_chr4B	641929_U:112608-114682
	4BL	60431_chr4A	308427_4AS:31581-32567
	4DL	71289_chr4D	342578_4DL:59,248-59,851

TABLE 3. Epitopes used for the production of monoclonal antibodies for asparagine synthetases TaASN1, TaASN2 and TaASN3 from wheat.

Protein	Epitope identified from GenBank entries	Corresponding sequence in TaASN1-3 from cv. Spark	Position in protein
TaASN1 (GenBank AY621539)	HLPATIMAGTSK	HLPAT <u>IL</u> TGTSK	558-569
	IMAGTSKKPRMI	<u>IL</u> TGTSKKPRMI	563-574
	SKKPRMIEVAAP	SKKPRMIEVAAP	568-579
	MIEVAAPGVAIES	MIEVAAPGVAIES	573-585
TaASN2 (GenBank BT009049)	TVAVGGSNKPGV	TVAVGGSNKPGV	558-569
	GGSNKPGVMNTV	GGSNKPGVMNTV	562-573
	KPGVMNTVVPGV	KPGVMNTVVPGV	566-577
	MNTVVPGVAIET	MNTVVPGVAIET	570-581
TaASN3 (GenBank AK333183)	KAPASADPVFRP	KAPAS <u>V</u> DP <u>V</u> LEN <u>A</u> FP	558-573
	DPVFRPPAHGES	DP <u>V</u> LEN <u>A</u> FP <u>P</u> AHGES	564-579
	PAHGESILVETG	PAHG <u>E</u> ST <u>L</u> V <u>K</u> SA	574-585
	ILVETGVPAAAV	<u>T</u> L <u>V</u> <u>K</u> SA <u>V</u> PAAAV	580-591

In review

TABLE 4. Rate parameters (mg/mL/s). Note that k_1 refers to reaction r_1 in the Petri net model shown in Figure 6, and likewise the other parameters, while k_D refers to the dissociation reaction D.

Rate parameter	TaASN1	TaAsn2
k_1	0.016	0.02
k_2	3	3
k_3	0.043	0.043
k_4	10	10
k_D	700	400

In review

FIGURE LEGENDS

FIGURE 1.

Amino acid sequence alignment of TaASN1, TaASN2 and TaASN3 proteins from wheat (*Triticum aestivum*) cv. Spark. Identical residues at the same position are highlighted in black, except for residues known to be critical for the function of the enzyme (see text), which are highlighted in red. Similar residues at the same position (conservative substitutions) are highlighted in grey. The region corresponding to peptides used to raise the two monoclonal antibodies that showed highest specificity for the asparagine synthetase proteins is indicated with a blue box.

FIGURE 2

Diagrammatic representation of the gene structures of *TaASN1*, *TaASN2*, *TaASN3.1*, *TaASN3.2* and *TaASN4*.

FIGURE 3

SDS polyacrylamide gel electrophoresis of extracts of *E. coli* cells expressing wheat asparagine synthetases: TaASN1, TaASN2 and TaASN3. Expression of the proteins was induced by addition of IPTG to the bacterial cell cultures. An uninduced control is included for each protein, and each protein is also shown after purification on a nickel-nitrilotriacetic acid (Ni-NTA) agarose column. The arrow indicates the position of the expressed proteins.

FIGURE 4

Western blot of heterologously-expressed TaASN1, TaASN2 and TaASN3 proteins reacted with monoclonal antibodies raised to peptides SKKPRMIEVAAP and GGSNKPGVMNTV, as indicated.

FIGURE 5

Plots (means with standard errors from two replicates) showing the synthesis of asparagine and glutamate, in reactions catalysed by TaASN1 (top) and TaASN2 (bottom).

FIGURE 6

Model representing the reaction catalysed by asparagine synthetase, comprising metabolites (circles), and reactions (squares). The concentration of metabolites is indicated abstractly by numbers in the circles. The model features eleven molecules: AMP, ATP, asparagine (Asn), glutamine (Gln), glutamate (Glu), aspartate (Asp), asparagine synthetase enzyme (ASNe), ASNe complexed with glutamine (ASNe-Gln), ASNe complexed with ammonia (ASNe-NH₃), β -aspartyl-complex (β Asp-AMP-ASNe-NH₃), and magnesium ions. Note that for clarity, water and pyrophosphate are not included. The model was generated assuming that the reactions follow mass action kinetics. The dissociation step for the ASNe-NH₃ complex is highlighted in red.

FIGURE 7

Time-series plots for parameter estimation against experimental data for TaASN1.

FIGURE 8

Time-series plots for parameter estimation against experimental data for TaASN2.

FIGURE 1

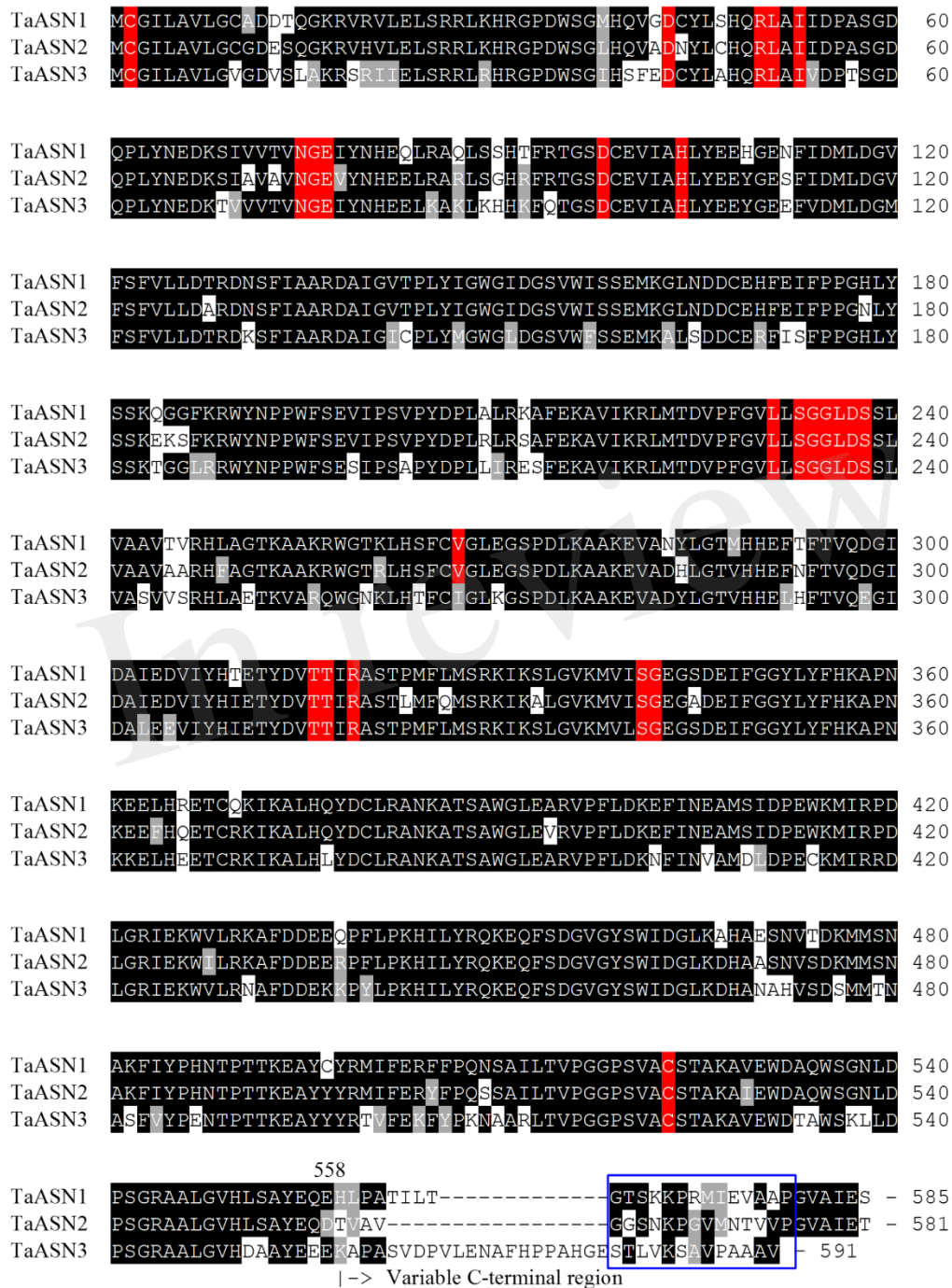
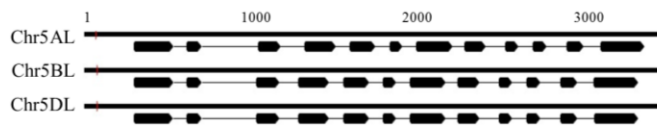
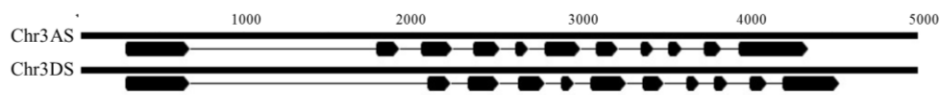


FIGURE 2

***TaASN1* on Chromosome 5**



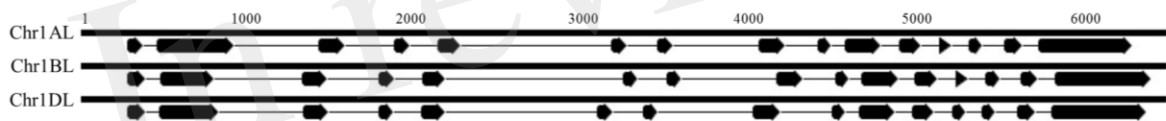
***TaASN2* on Chromosome 3**



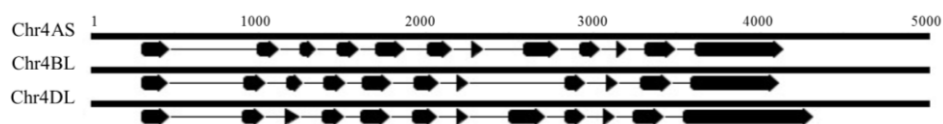
***TaASN3.1* on Chromosome 1**



***TaASN3.2* on Chromosome 1**



***TaASN4* on Chromosome 4**



Key: Exon Intron

FIGURE 3

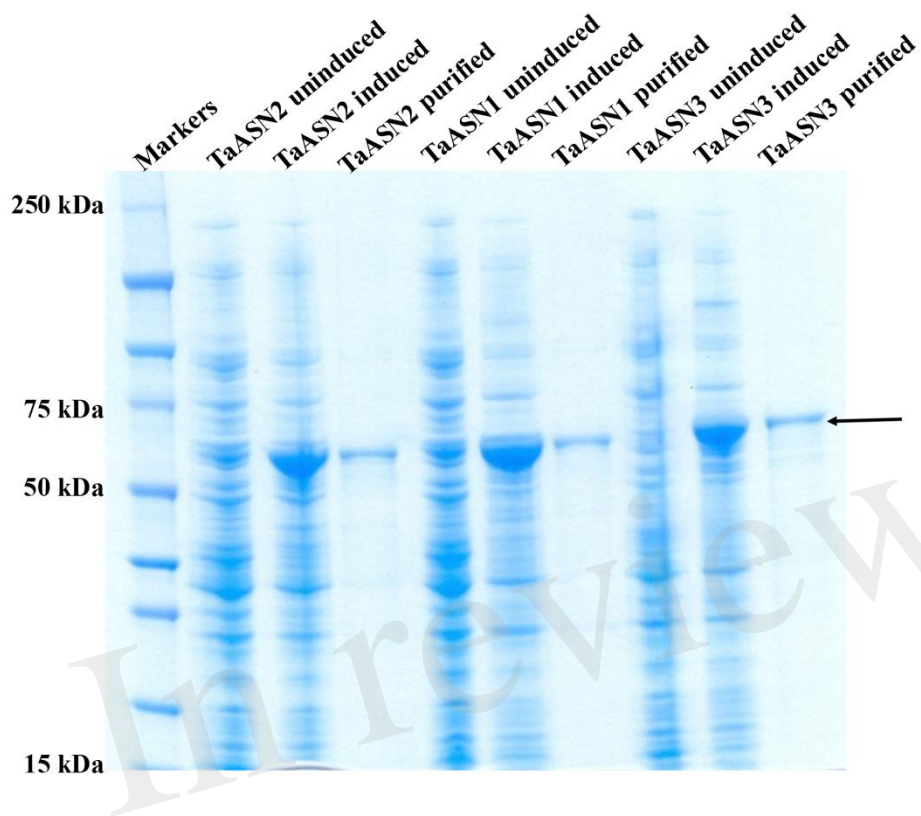


FIGURE 4

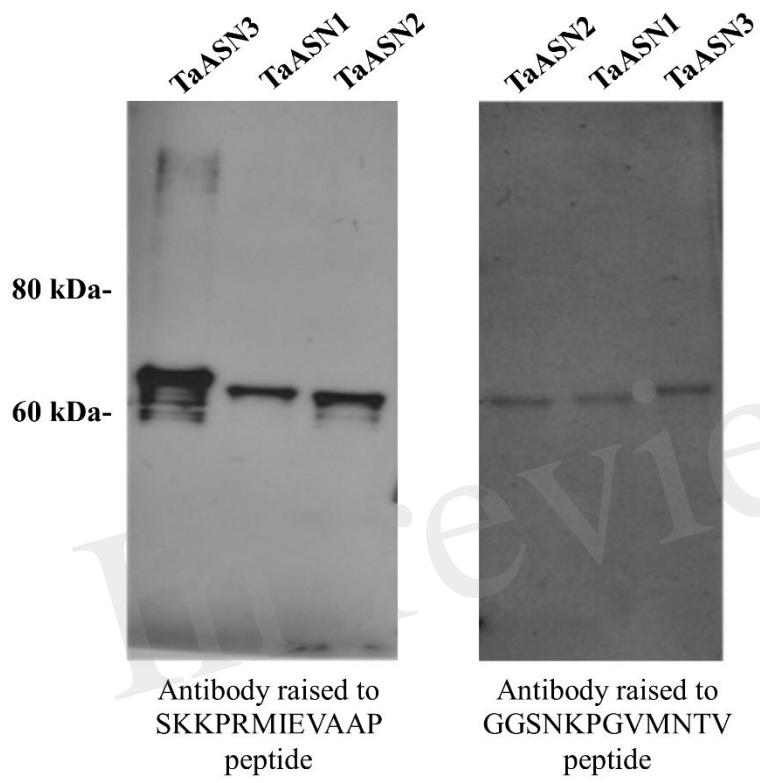


FIGURE 5

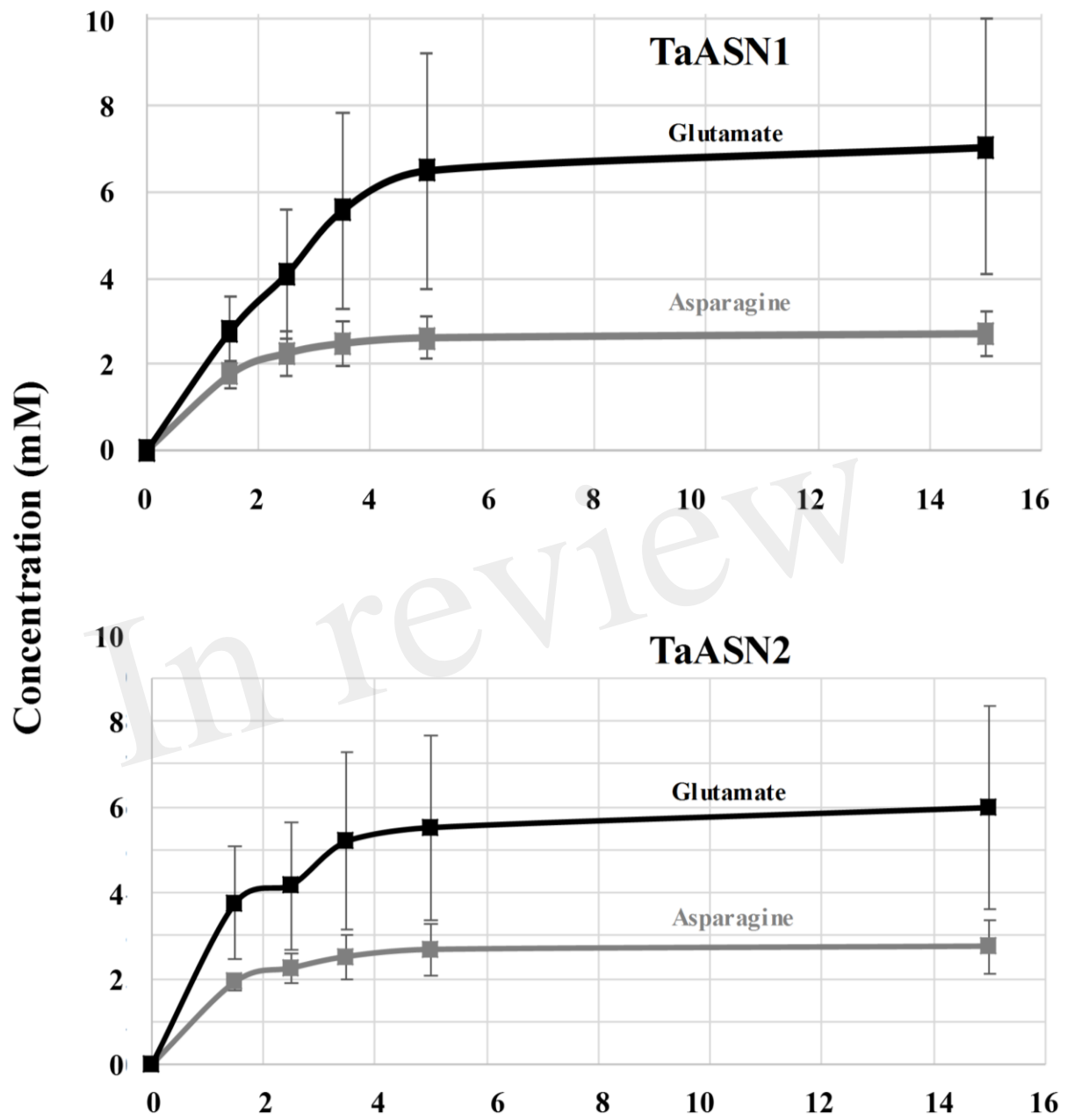
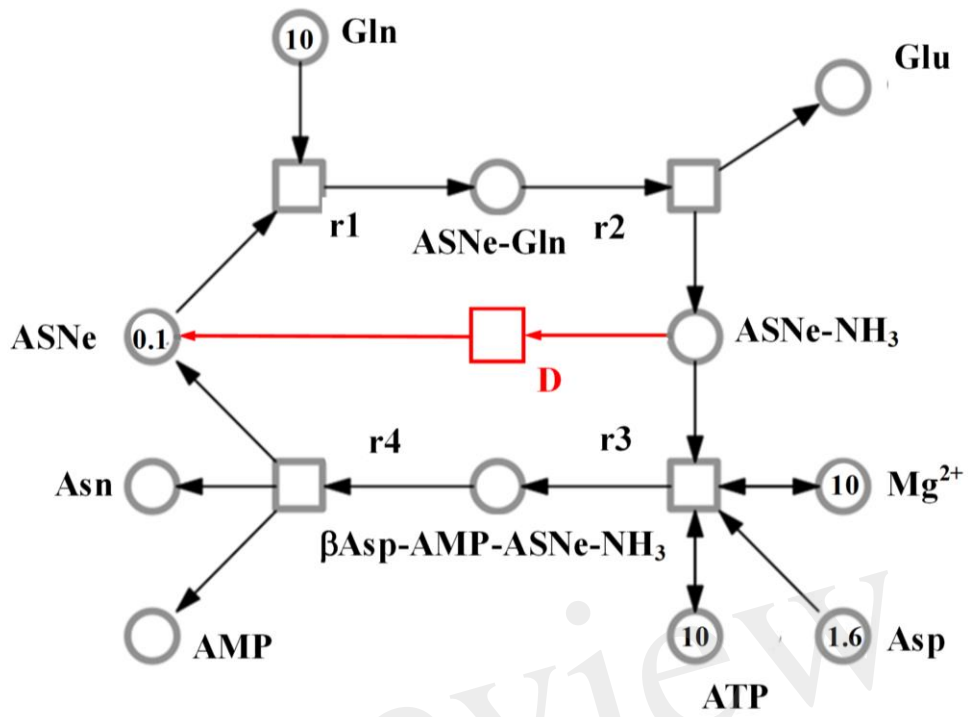


FIGURE 6



In review

FIGURE 7

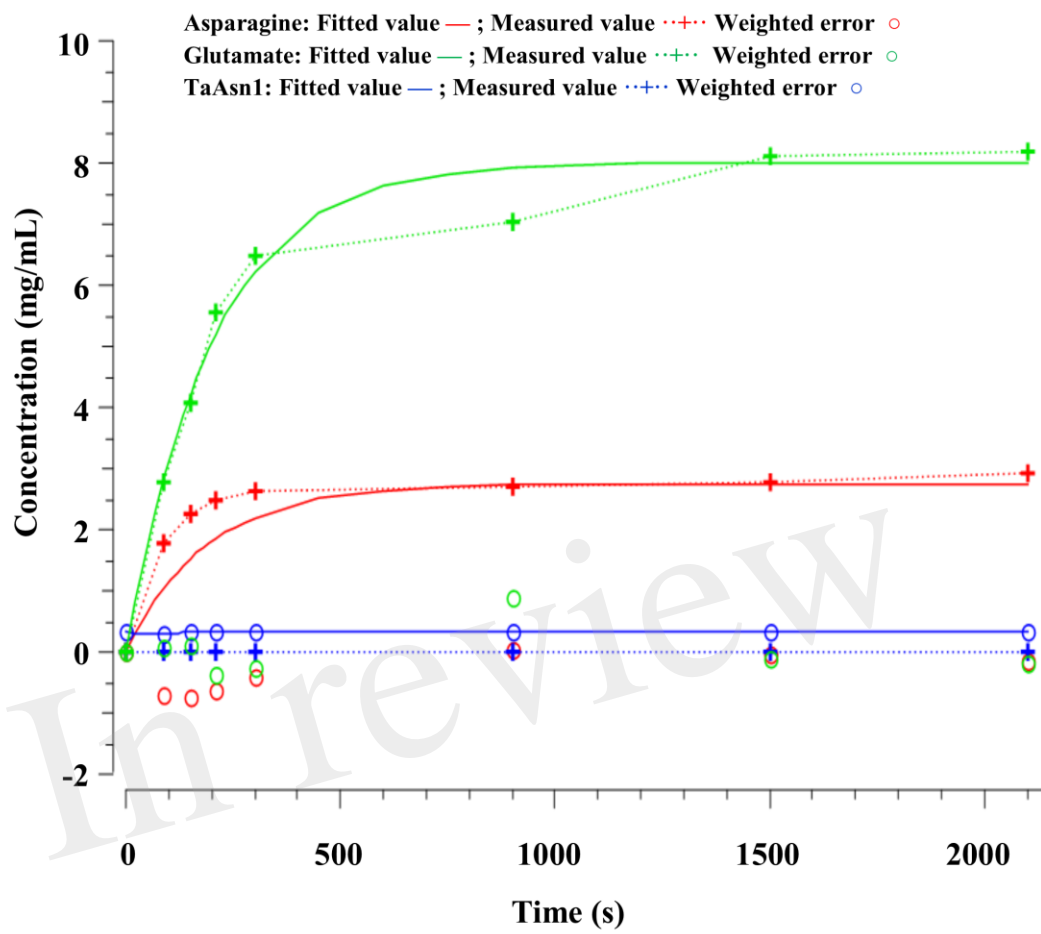


FIGURE 8

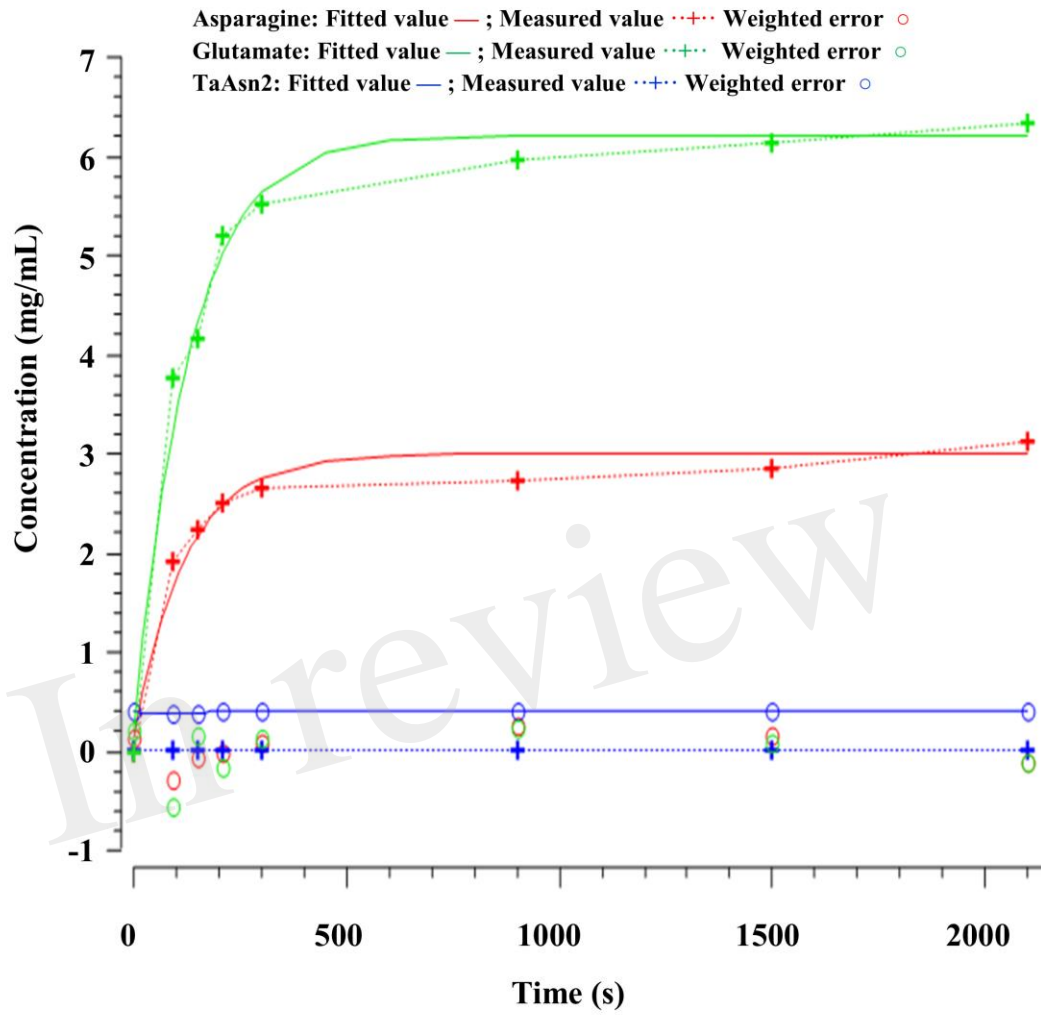


Figure 1.TIF

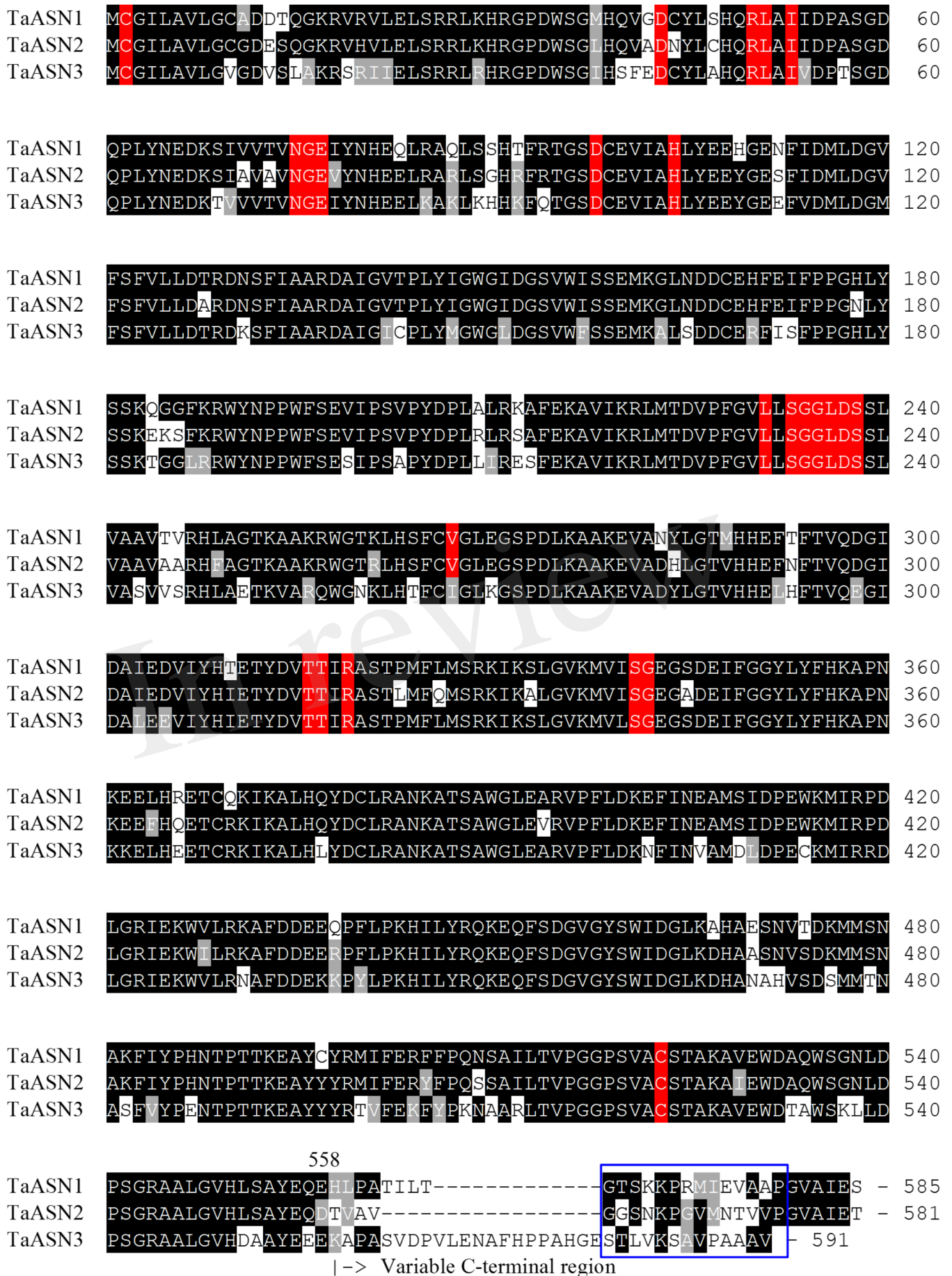
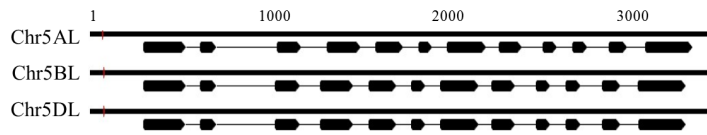


Figure 2.TIF

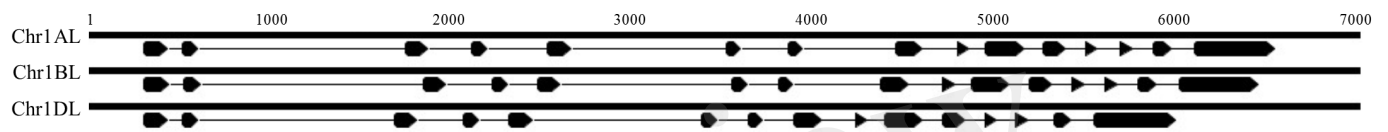
TaASN1 on Chromosome 5



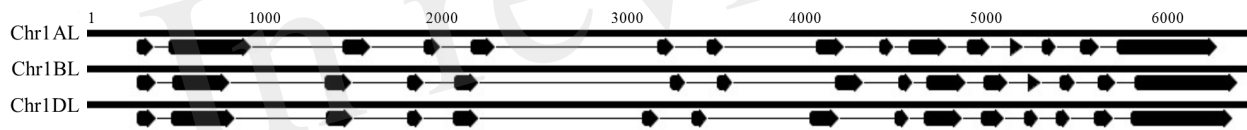
TaASN2 on Chromosome 3



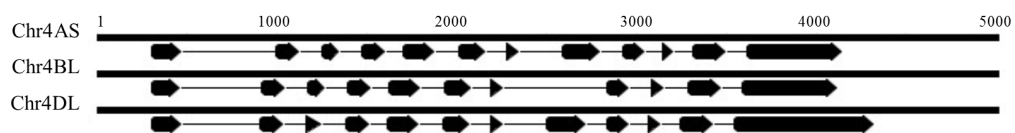
TaASN3.1 on Chromosome 1



TaASN3.2 on Chromosome 1



TaASN4 on Chromosome 4



Key: Exon Intron

Figure 3.TIF

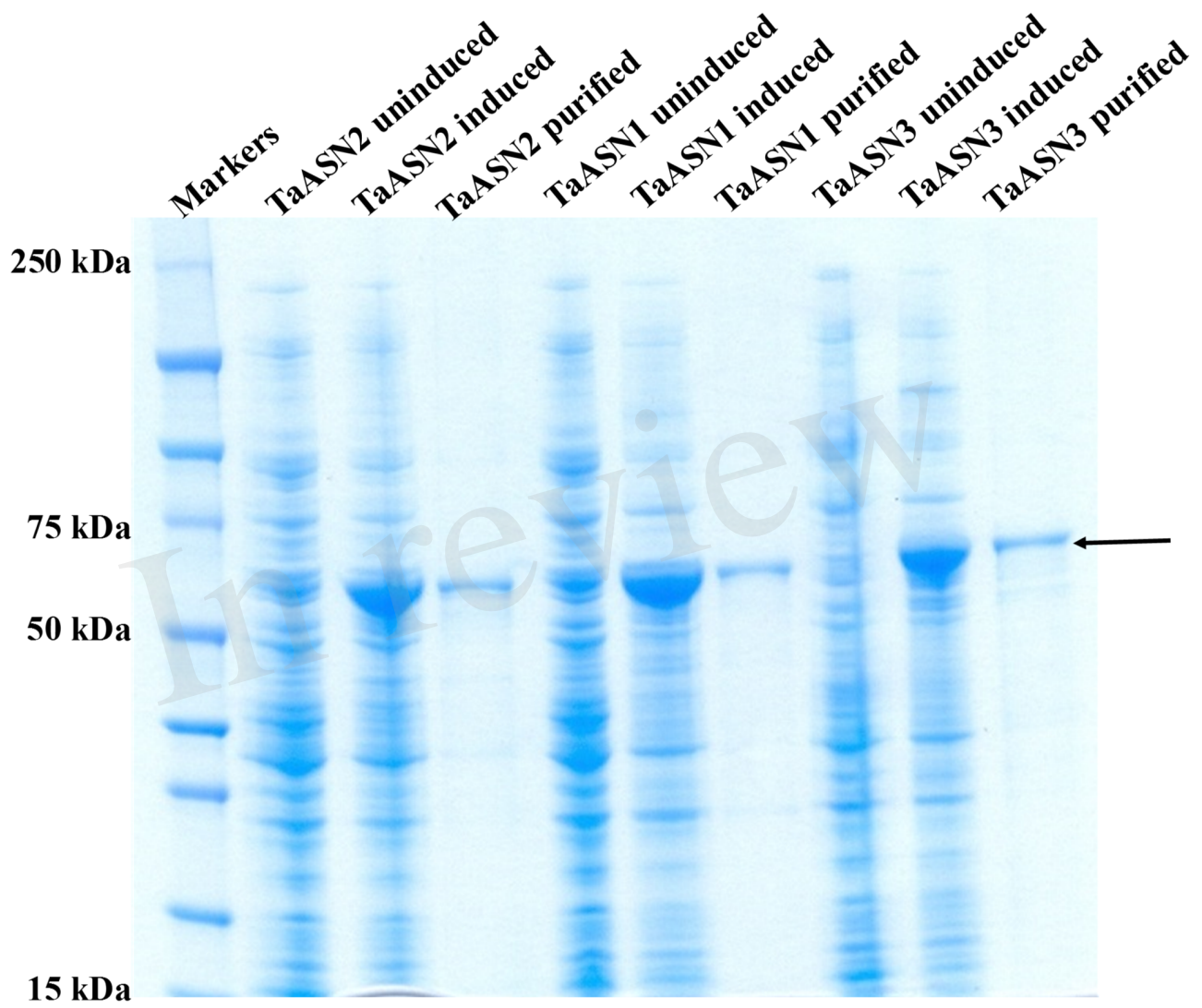


Figure 4.TIF

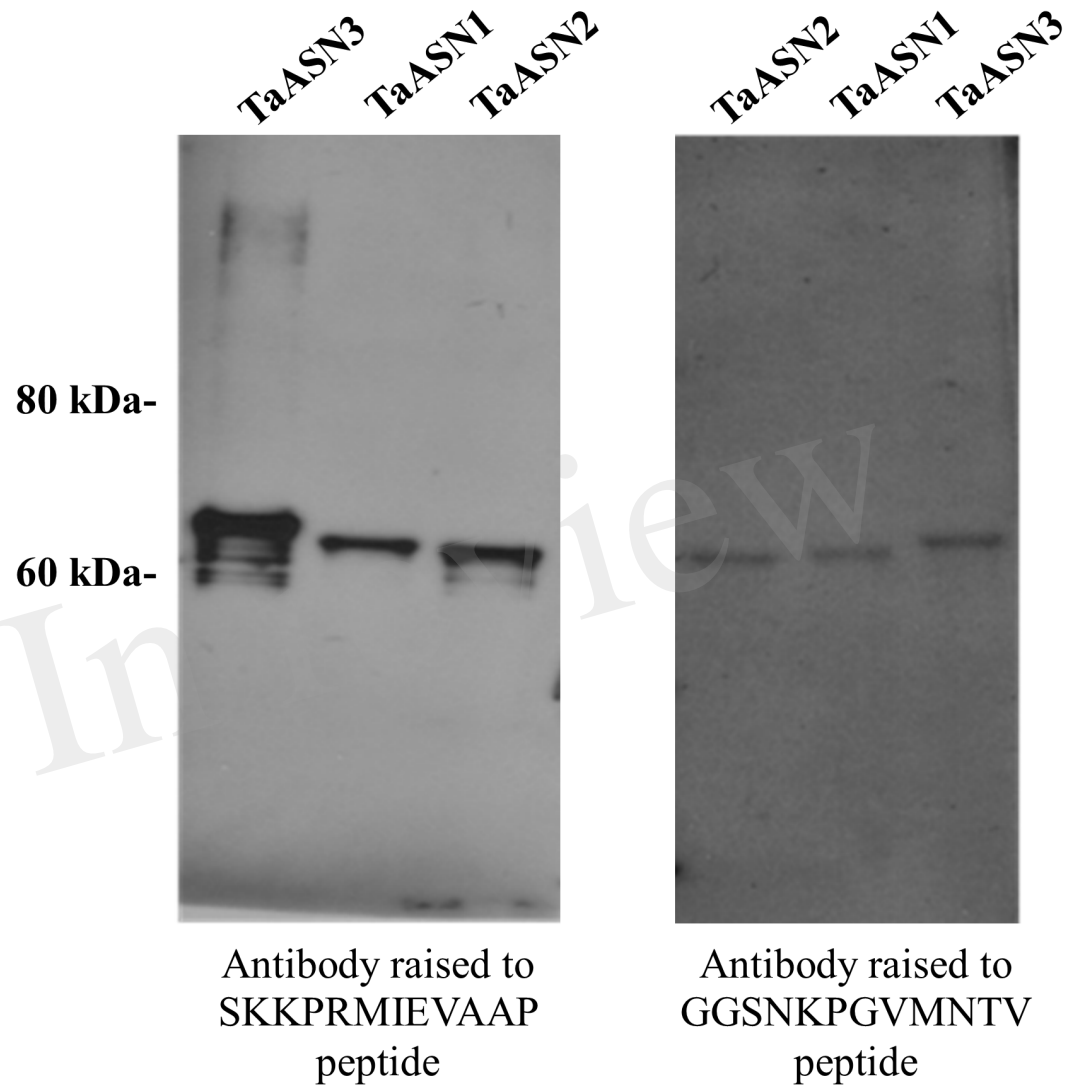


Figure 5.TIF

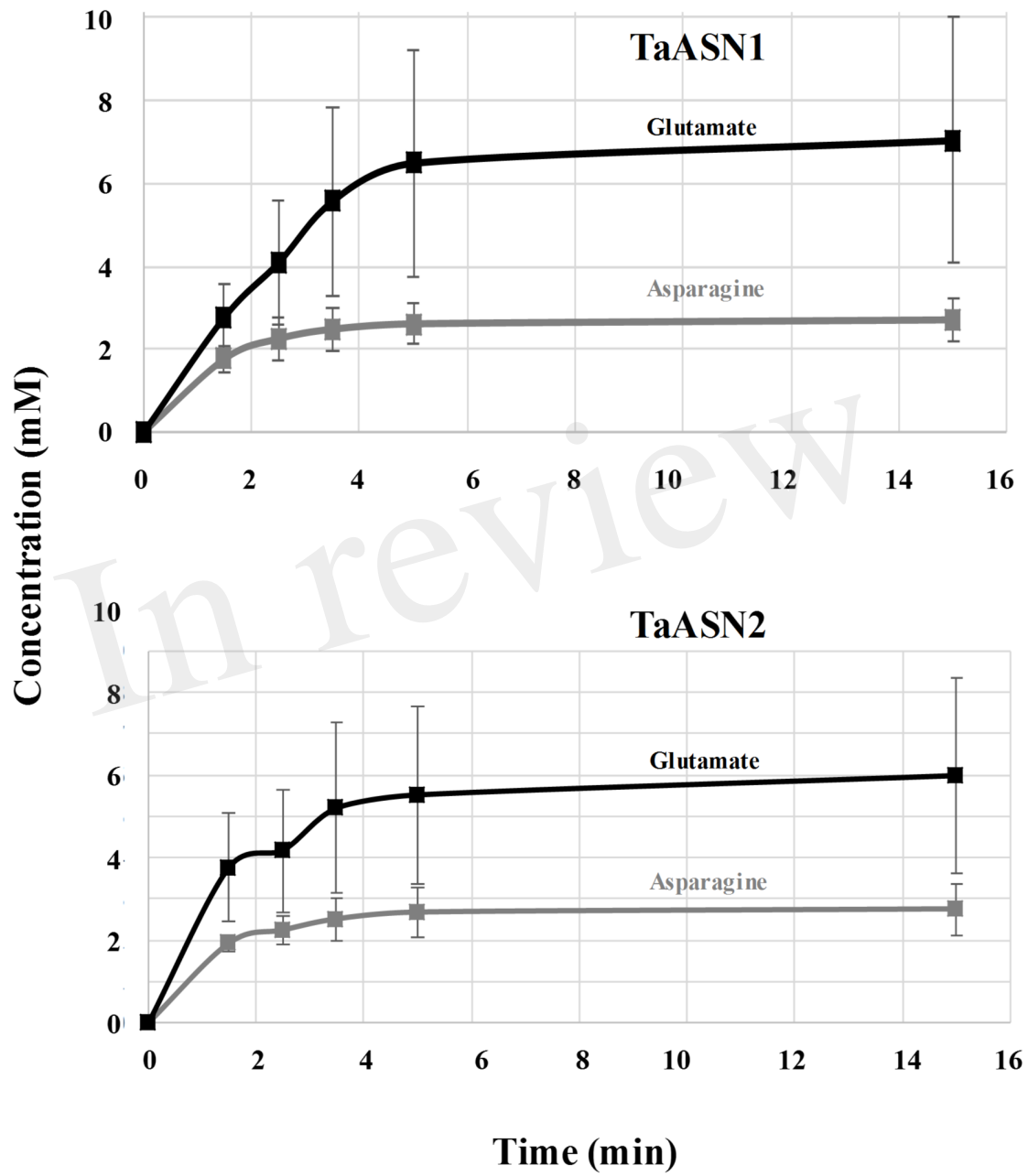


Figure 6.TIF

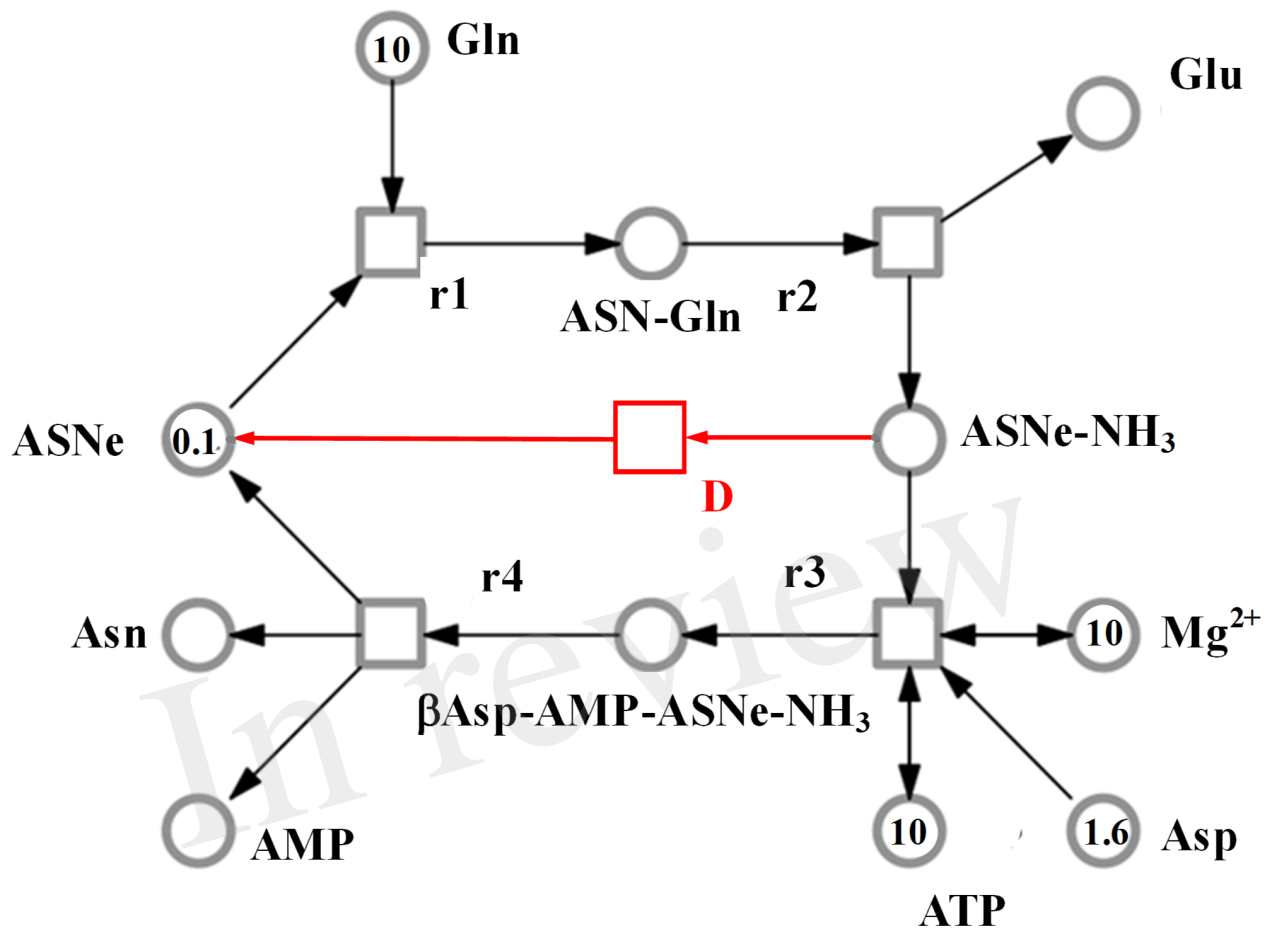


Figure 7.TIF

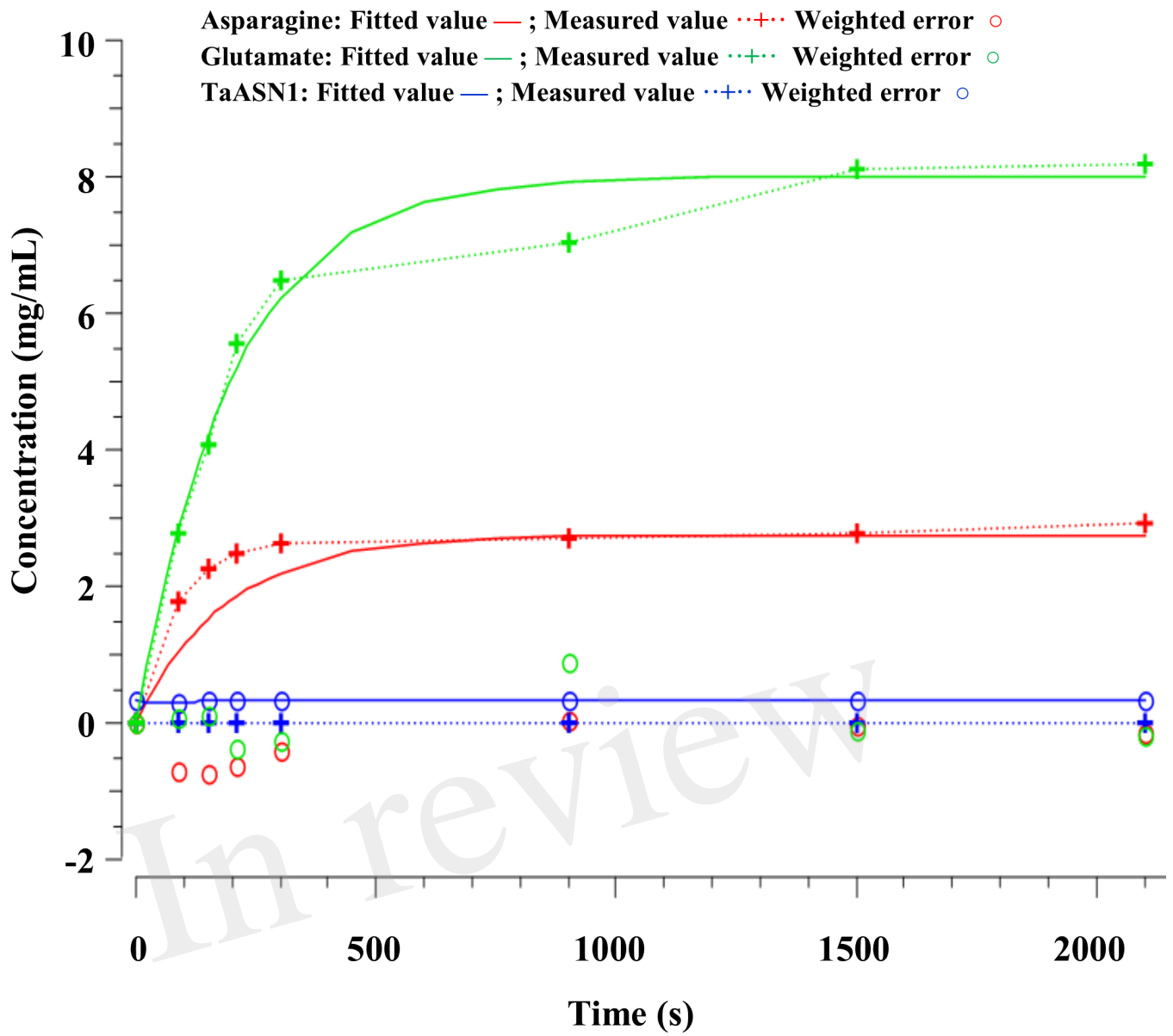


Figure 8.TIF

